



**HAL**  
open science

## Mapping the spatial distribution of global $^{137}\text{Cs}$ fallout in soils of South America as a baseline for Earth Science studies

Pierre-Alexis Chaboche, Nicolas Saby, J. Patrick Laceby, Jean P.G. Minella, Tales Tiecher, Rafael Ramon, Marcos Tassano, Pablo Cabral, Mirel Cabrera, Yuri Jacques Agra Bezerra da Silva, et al.

### ► To cite this version:

Pierre-Alexis Chaboche, Nicolas Saby, J. Patrick Laceby, Jean P.G. Minella, Tales Tiecher, et al.. Mapping the spatial distribution of global  $^{137}\text{Cs}$  fallout in soils of South America as a baseline for Earth Science studies. *Earth-Science Reviews*, 2021, 214, pp.103542. 10.1016/j.earscirev.2021.103542 . cea-03128666

**HAL Id: cea-03128666**

**<https://cea.hal.science/cea-03128666>**

Submitted on 4 Feb 2021

**HAL** is a multi-disciplinary open access archive for the deposit and dissemination of scientific research documents, whether they are published or not. The documents may come from teaching and research institutions in France or abroad, or from public or private research centers.

L'archive ouverte pluridisciplinaire **HAL**, est destinée au dépôt et à la diffusion de documents scientifiques de niveau recherche, publiés ou non, émanant des établissements d'enseignement et de recherche français ou étrangers, des laboratoires publics ou privés.

1 **Mapping the spatial distribution of global <sup>137</sup>Cs fallout in soils of South America as a baseline for**  
2 **Earth Science studies**

3 Pierre-Alexis Chaboche<sup>1\*</sup>, Nicolas P.A. Saby<sup>2</sup>, J. Patrick Lacey<sup>3</sup>, Jean P.G. Minella<sup>4</sup>, Tales Tiecher<sup>5</sup>,

4 Rafael Ramon<sup>1,6</sup>, Marcos Tassano<sup>7</sup>, Pablo Cabral<sup>7</sup>, Mirel Cabrera<sup>7</sup>, Yuri Jacques Agra Bezerra da Silva<sup>8</sup>,

5 Irène Lefevre<sup>1</sup>, Olivier Evrard<sup>1</sup>

6 <sup>1</sup>Laboratoire des Sciences du Climat et de l'Environnement (LSCE/IPSL), Unité Mixte de Recherche 8212 (CEA-  
7 CNRS-UVSQ), Université Paris-Saclay, Gif-sur-Yvette, France

8 <sup>2</sup>INRAE, Unité Infosol US1106, Orléans 2, France

9 <sup>3</sup>Alberta Environment and Parks, 3535 Research Rd NW Calgary, Alberta, Canada, T2L 2K8, Canada

10 <sup>4</sup>Department of Soils, Federal University of Santa Maria, 97105-900 Santa Maria, Brazil

11 <sup>5</sup> Department of Soil Science, Federal University of Rio Grande do Sul, Bento Gonçalves Ave. 7712, 91540-000  
12 Porto Alegre, RS, Brazil

13 <sup>6</sup> Graduate Program in Soil Science, Federal University of Rio Grande do Sul, Bento Gonçalves Ave., 91540-000  
14 Porto Alegre, RS, Brazil

15 <sup>7</sup>Laboratorio de Radioquímica, Centro de Investigaciones Nucleares, Facultad de Ciencias, Universidad de la  
16 República, Montevideo, Uruguay.

17 <sup>8</sup>Agronomy Department, Federal University of Piauí (UFPI), Planalto Horizonte, 64900-000, Bom Jesus, PI, Brazil

18 **\*Corresponding author.** Tel.: +33 1 69 08 35 99

19 E-mail address: [pierre-alexis.chaboche@lsce.ipsl.fr](mailto:pierre-alexis.chaboche@lsce.ipsl.fr)

20 Present address : *LSCE (Laboratoire des Sciences du Climat et de l'Environnement), UMR 8212 (CEA-  
21 CNRS-UVSQ), Université Paris-Saclay, l'Orme des Merisiers 91191 Gif-sur-Yvette Cedex (France)*

22

23

24

25 **Abstract**

1  
2  
3 26 Owing to the rapid expansion of agriculture in South America in recent decades, soil erosion and fine  
4  
5 27 sediment supply to river networks, which lead to deleterious on-site and off-site environmental  
6  
7 28 impacts, are exacerbated in intensively cultivated catchments. Measuring soil inventories of bomb-  
8  
9  
10 29 derived fallout radiocesium ( $^{137}\text{Cs}$ ) bound to fine particles is one of the few techniques available to  
11  
12 30 reconstruct soil redistribution rates and evaluate the sustainability of farming practices over the recent  
13  
14 31 phase of agricultural intensification (1960s–2020). However, information about the spatial distribution  
15  
16 32 of  $^{137}\text{Cs}$  fallout across the soils of South America remains scarce, and the published data has not been  
17  
18 33 synthesized at the scale of this subcontinent so far. The objective of the current research is therefore  
19  
20  
21 34 to quantify and map the initial  $^{137}\text{Cs}$  fallout at the scale of South America, based on the compilation of  
22  
23 35 published  $^{137}\text{Cs}$  inventories, additional measurements conducted on undisturbed soil profiles and  
24  
25 36 digital soil mapping as this baseline information may be useful for a wide range of Earth Science  
26  
27 37 applications. A database of  $^{137}\text{Cs}$  inventories at 96 reference sites (i.e. areas without soil erosion nor  
28  
29  
30 38 accumulation) has been compiled for a variety of soil profiles (Argentina = 10, Brazil = 34, Chile = 46,  
31  
32 39 Uruguay = 5, French Guiana = 1) located between 5.3° North latitude and 53° South latitude. The spatial  
33  
34 40 distribution of  $^{137}\text{Cs}$  fallout was shown to be highly latitude-dependent, with a maximum in the 30-50°  
35  
36 41 South latitude band. There were higher fallout levels than expected between 20 to 60° South latitude  
37  
38  
39 42 compared to the previous estimations made by UNSCEAR. A partial least square regression approach  
40  
41 43 based on rainfall data and geographical information as covariates was used to create a baseline map  
42  
43 44 of  $^{137}\text{Cs}$  fallout in soils of continental South America. This baseline map provides a powerful reference  
44  
45 45 dataset to anticipate the order of magnitude of  $^{137}\text{Cs}$  inventories in undisturbed soil profiles collected  
46  
47 46 in Brazil and Southern Chile and for numerous other applications in Earth Sciences. The potential  
48  
49  
50 47 application of the  $^{137}\text{Cs}$  inventory technique in countries of South America in general, and in regions  
51  
52 48 with vulnerable ecosystems threatened by the expansion of agricultural activities in particular, is  
53  
54 49 discussed in light of this comprehensive literature review. Furthermore, the regions (i.e. the North-  
55  
56 50 Western part of the continent) where additional samples should be collected in priority to improve  
57  
58  
59 51 this baseline map are outlined. Our results demonstrate that  $^{137}\text{Cs}$  inventories are sufficiently high to  
60  
61  
62  
63  
64  
65

1  
2  
3  
4  
52 investigate soil redistribution rates in most of South American countries where detectable levels of  
53  $^{137}\text{Cs}$  can be expected to be found in sites exposed to erosion.

54 **Keywords:** Digital soil mapping, Caesium-137, Soil erosion, Soil redistribution rates, Reference soil sites  
55

## 56 **1. Introduction**

57

58 Soil is essentially a non-renewable resource over the human timescale (Lal, 2015). The future use of  
59 this valuable resource is threatened by anthropogenic activities such as the intensification of  
60 agricultural practices (Keesstra et al., 2016). The Great Acceleration period that started during the  
61 second half of the 20<sup>th</sup> century induced a significant increase of soil erosion and degradation (Steffen  
62 et al., 2015), leading to extensive on-site and off-site impacts. On-site, soil erosion threatens soil  
63 fertility and agricultural yields (Bakker et al., 2007; Bakker et al., 2004; Vanwalleghem et al., 2017).  
64 Fine-grained sediment transported off-site, which may be associated with nutrients and contaminants,  
65 leads to the reduction of water quality, the degradation of aquatic habitats and reservoir siltation  
66 (Becker et al., 2009; Evrard et al., 2007; Foucher et al., 2014). Fine sediment supply induced by soil  
67 erosion processes is exacerbated in intensively cultivated catchments, leading to deleterious  
68 consequences for river systems (Owens et al., 2005) and to the disturbance of global biogeochemical  
69 cycles (Quinton et al., 2010).

70 In order to evaluate the sustainability of agricultural practices and promote effective soil management  
71 practices, a fundamental prerequisite is to quantify soil erosion rates. Measuring soil inventories of  
72 fallout radionuclide Caesium-137 ( $^{137}\text{Cs}$ ,  $t_{1/2} = 30.2$  years) has shown great potential to provide  
73 retrospective information on soil redistribution rates over the medium-term (Ritchie and Ritchie,  
74 2007), despite the critiques made on this method (Parsons and Foster, 2011). The latter authors  
75 recommended that future studies should present their results in light of the underlying hypotheses  
76 (e.g. the spatial uniformity of fallout at the local scale). Despite the ongoing debate in the literature,

1  
2  
3  
4  
5  
6  
7  
8  
9  
10  
11  
12  
13  
14  
15  
16  
17  
18  
19  
20  
21  
22  
23  
24  
25  
26  
27  
28  
29  
30  
31  
32  
33  
34  
35  
36  
37  
38  
39  
40  
41  
42  
43  
44  
45  
46  
47  
48  
49  
50  
51  
52  
53  
54  
55  
56  
57  
58  
59  
60  
61  
62  
63  
64  
65

77 this technique has been increasingly adopted as a field-based approach to quantify soil erosion or  
78 deposition since the 1980s in several catchments around the world (Chartin et al., 2013; Fukuyama et  
79 al., 2005; Mabit et al., 2018; Mabit et al., 2008; Navas et al., 2005; Zapata, 2002).

80 <sup>137</sup>Cs is an artificial radionuclide generated as a product of the atmospheric nuclear weapon tests  
81 carried out between 1945 and 1980, or released by nuclear accidents (e.g. Chernobyl in Ukraine,  
82 Fukushima in Japan) (Steinhauser et al., 2014). The introduction of <sup>137</sup>Cs into the global environment  
83 also coincides with the transformation of farming practices initiated in the 1960s through the  
84 increasing use of external inputs and heavy machinery (Camargo et al., 2017). When deposited onto  
85 the soil surface, <sup>137</sup>Cs is rapidly and almost irreversibly bound to fine particles, as its desorption by the  
86 natural chemical processes infrequently occurs in continental environments (Tamura, 1961; Tamura  
87 and Jacobs, 1960). Assessment of erosion and deposition rates is commonly based on the comparison  
88 of <sup>137</sup>Cs inventories (Bq m<sup>-2</sup>) in undisturbed soil profiles with those inventories measured at locations  
89 affected by soil redistribution in the landscape (Loughran et al., 2002; Walling and Quine, 1990). A  
90 reference site is defined as an undisturbed soil profile where neither erosion nor deposition has  
91 occurred since the period of radioactive fallout. Accordingly, it contains the cumulative atmospheric  
92 fallout input at the site reduced by radioactive decay only (Zapata, 2003). Measuring <sup>137</sup>Cs inventories  
93 in reference sites may therefore provide the only indirect approach available nowadays to reconstruct  
94 the initial fallout released by the nuclear weapon tests on these soils.

95 Understanding the spatial distribution of initial <sup>137</sup>Cs fallout is important for several scientific  
96 disciplines, including medical science (Gilbert et al., 2002; McCarthy, 1997; Simon et al., 2006) as well  
97 as various fields in Earth Science, with applications in ocean, atmosphere and soil-related studies  
98 (Buesseler and Benitez, 1994; Ehhalt, 1973; Jagercikova et al., 2017). The first estimation of the fallout  
99 spatial pattern was made by the United Nations Scientific Committee of the Effects of Atomic Radiation  
100 (UNSCEAR, 1962) in order to evaluate the health hazard of fallout radionuclides. Based on the results  
101 of a long-term monitoring programme of global fallout deposition, a uniform distribution model for

102 10-degree latitudinal bands was established in the UNSCEAR report published in 2000. In parallel, soil  
1 erosion and soil-to-crop transfer studies have provided more accurate local information on the spatial  
2 103  
3 distribution of initial  $^{137}\text{Cs}$  fallout worldwide (Owens and Walling, 1996; Ritchie and McHenry, 1990;  
4 104  
5 Walling and He, 2000). The deposition of fallout radionuclides onto the Earth surface is conditioned by  
6 105  
7 two major factors: latitude and rainfall. Ground deposition of radionuclides from the global fallout was  
8 106  
9 shown to be highly latitude-dependent, with a maximum in the 40-50° bands in both hemispheres  
10 107  
11 (UNSCEAR, 2000). In addition, the activity of  $^{137}\text{Cs}$  deposited on the ground and its variation from one  
12 108  
13 location to another is closely linked to the annual rainfall rates, as a consequence of precipitation  
14 109  
15 scavenging (Bouisset et al., 2018; La Manna et al., 2019; Le Roux et al., 2010; Malakhov and Pudovkina,  
16 110  
17 1970). Moreover, relationships between monthly rainfall rates and  $^{90}\text{Sr}$  fallout were observed in South  
18 111  
19 America, with a peak during the months of June-August (Volchok, 1965; Volchok, 1966). Based on these  
20 112  
21 two factors, digital mapping using geostatistical approaches has been conducted at different scales to  
22 113  
23 map bomb-derived  $^{137}\text{Cs}$  fallout (Almgren et al., 2006; Aoyama et al., 2006; Chappell et al., 2011a;  
24 114  
25 Furuichi and Wasson, 2013; Meusburger et al., 2020; Palsson et al., 2006). Although reconstructions  
26 115  
27 of baseline  $^{137}\text{Cs}$  inventories were made for Europe, Australia and Eastern Asia, information about the  
28 116  
29 spatial distribution of  $^{137}\text{Cs}$  in soils of South America remains scarce, which requires further  
30 117  
31 investigation to determine the potential for application of  $^{137}\text{Cs}$  for Earth Science studies in this  
32 118  
33 subcontinent. Of note, the  $^{137}\text{Cs}$  inventories in soils of the Southern hemisphere are usually sufficient  
34 119  
35 to be measurable by gamma spectrometry when using appropriate low-background detectors during  
36 120  
37 sufficient counting times (FAO/IAEA, 2017).

48 122 Quantifying  $^{137}\text{Cs}$  inventories in soils and calculating the corresponding soil redistribution rates during  
49 123  
50 the intensive cultivation period (1960 to present) is particularly important to evaluate the sustainability  
51 124  
52 of agricultural practices implemented in South America during the last several decades to maintain  
53 125  
54 erosion at sustainable levels (Minella et al., 2014). During the last 50 years, most countries of the  
55 126  
56 subcontinent have abandoned conventional tillage to implement no-till farming (Montgomery, 2007).  
57 127  
58 This change in practice has been accompanied by an increase in the size of cultivated areas and their  
59  
60

128 overall productivity (Wingeyer et al., 2015). However, no-till farming has been widely implemented as  
129 a single conservation measure without additional practices to reduce soil loss, such as crop rotation or  
130 contour cropping and terracing (Didone et al., 2019; Montgomery, 2007). As a consequence, soil  
131 erosion by water remains the main soil degradation process in agricultural land of South America and  
132 its real magnitude remains debated among agricultural and scientific communities (FAO, 2015).

133 To provide independent estimations of soil redistribution rates, appropriate reference soil sites are  
134 increasingly difficult to find in these intensive agricultural areas, given the growing extent of crops on  
135 almost all available land areas. The indirect estimation of  $^{137}\text{Cs}$  inventories in reference soil sites of  
136 South America is therefore required to assess soil redistribution rates with the  $^{137}\text{Cs}$  technique. Based  
137 on the compilation of published  $^{137}\text{Cs}$  inventories and additional measurements conducted on  
138 undisturbed soil profiles, the primary goals of this study are (1) to present and discuss the spatial  
139 distribution of  $^{137}\text{Cs}$  inventories in reference soil sites across South America, (2) to map the initial  $^{137}\text{Cs}$   
140 fallout at the scale of South America using a digital mapping approach in order to provide estimates at  
141 unsampled reference locations, and (3) discuss the potential for application of this technique and other  
142 Earth Science approaches in countries of South America. Although this new map cannot replace the  
143 sampling of profiles in local reference areas, it will provide useful information for guiding and designing  
144 future Earth Science studies in South America using  $^{137}\text{Cs}$  global fallout.

145

## 2. Spatial distribution of bomb-derived $^{137}\text{Cs}$ in soils of South America

### 2.1. Global fallout following nuclear weapon tests

152 The UNSCEAR reports provide the main source of information regarding  $^{137}\text{Cs}$  deposition worldwide.  
153 Early studies about the production and transport of nuclear weapon debris started in 1962 (UNSCEAR,  
154 1962). It is currently accepted that a total of 502 atmospheric tests, with a total fission and fusion yield

155 of 440 Mt, were conducted from the mid-1950s to 1980 (UNSCEAR, 2008). Following the extensive  
1 tests of atmospheric nuclear devices in 1962, the deposition of <sup>137</sup>Cs reached a peak in 1963 and 1965  
2 156 tests of atmospheric nuclear devices in 1962, the deposition of <sup>137</sup>Cs reached a peak in 1963 and 1965  
3  
4 157 in the Northern and Southern hemispheres, respectively (Cambray et al., 1989; Turney et al., 2018).  
5  
6  
7 158 The signing of the Partial Test-Ban Treaty on August 5, 1963 by the United Kingdom, the Soviet Union  
8  
9 159 and the United States has contributed to the reduction of global emissions of artificial radionuclides  
10  
11 160 into the environment. In soils of South America, no trace of Chernobyl and Fukushima Daichii-derived  
12  
13 161 fallout radionuclides were detected, which makes the atmospheric weapon test fallout the single  
14  
15 162 significant source of artificial radioactivity in this part of the world (Steinhauser et al., 2014).  
16  
17  
18  
19 163 The radioactive debris emitted as a result of atmospheric nuclear tests were distributed between the  
20  
21 164 surface of the ground or water and the tropospheric and stratospheric regions, depending on the type  
22  
23 165 of test (offshore barge, top of a tower, under a tethered balloon, etc.), the location (altitude and firing  
24  
25 166 latitude) and the power (kilotonnic or megatonnic). The majority of the radioactive debris was  
26  
27 167 dispersed into the stratosphere (referred to as “stratospheric fallout” or “global” fallout). The activity  
28  
29 168 that did not reach the stratosphere is referred to as “local / regional” fallout and “tropospheric fallout”  
30  
31 169 (UNSCEAR, 2000).  
32  
33  
34  
35  
36 170 Local fallout includes radioactive aerosol particles generally larger than 50 µm in size that are  
37  
38 171 deposited within a radius of about 100 km from the epicentre of the explosion (Garcia Agudo, 1998).  
39  
40 172 Tropospheric fallout is characterized by smaller aerosols that were deposited with a mean atmospheric  
41  
42 173 residence time of up to 30 days. During this period, the debris were dispersed within the latitude band  
43  
44 174 of the initial injection and followed wind-driven trajectories, before falling to the ground as a  
45  
46 175 consequence of precipitation scavenging (Bennett, 2002). Stratospheric fallout, which makes up a large  
47  
48 176 portion of total deposition, consists of particles that are transported into the stratosphere, dispersed  
49  
50 177 and then deposited globally, most of which occurs in the hemisphere of the initial injection.  
51  
52 178 Stratospheric deposition accounts for the majority of global long-lived fission product residues  
53  
54 179 (UNSCEAR, 2000).  
55  
56  
57  
58  
59  
60  
61  
62  
63  
64  
65

180 In order to estimate radionuclide deposition following nuclear detonations, two long-term monitoring  
1  
2 181 programmes were established during the nuclear weapon test period. The first programme, conducted  
3  
4 182 by the United Kingdom Atomic Energy Authority (UKAEA) consisted of 8 stations located in the United  
5  
6  
7 183 Kingdom and 18 stations installed in the rest of the world. The second programme, conducted by the  
8  
9 184 Environmental Measurements Laboratory in the United States (EML), as early as in 1954, consisted of  
10  
11 185 177 stations distributed worldwide. This monitoring programme, based on monthly  $^{90}\text{Sr}$  fallout  
12  
13  
14 186 sampling, was the largest and the most widely distributed and therefore, it has been adopted by the  
15  
16 187 UNSCEAR to estimate the total hemispheric annual deposition of  $^{90}\text{Sr}$  (UNSCEAR, 1993). The global  
17  
18 188 distribution of  $^{137}\text{Cs}$  was assessed assuming a  $^{137}\text{Cs}/^{90}\text{Sr}$  fission yield ratio of 1.5, and a uniform  
19  
20  
21 189 distribution model for each 10-degree latitude band was published in the UNSCEAR (2000) report.

22  
23  
24 190 The latitudinal distribution of  $^{137}\text{Cs}$  described by UNSCEAR should be taken with caution as 50% of the  
25  
26 191 data is missing from this monitoring programme (Evrard et al., 2020). Indeed, a significant proportion  
27  
28  
29 192 of data is lacking for monitoring stations ( $n=34$ ) located in South America. In all, 59% of monthly  $^{90}\text{Sr}$   
30  
31 193 fallout data is missing between 1954-1976, as most of the monitoring stations did not have continuous  
32  
33 194 records (Health and Safety Laboratory, 1977). In addition, when studies investigating  $^{137}\text{Cs}$  inventories  
34  
35  
36 195 in undisturbed soil profiles are conducted at regional or continental scales, the proportion of global  
37  
38 196 fallout estimated by UNSCEAR appears to be underestimated (Aoyama et al., 2006; Chappell et al.,  
39  
40  
41 197 2011a; Schuller et al., 2002; Tagami et al., 2019). Regarding the information currently available for  $^{137}\text{Cs}$   
42  
43 198 fallout at the scale of South America, the only reference is a study published by Garcia Agudo (1998)  
44  
45 199 who also used results of these monitoring programmes to map the global inventory of  $^{137}\text{Cs}$  from  
46  
47  
48 200 nuclear tests worldwide. Given the wide range of applications of  $^{137}\text{Cs}$  in the scientific literature, as  
49  
50 201 well as the debate raised on its use as a tracer for soil erosion assessment (Mabit et al., 2013; Parsons  
51  
52 202 and Foster, 2011; Parsons and Foster, 2013), a more accurate characterization of the initial fallout of  
53  
54  
55 203 bomb-derived  $^{137}\text{Cs}$  and its spatial distribution across South America is fundamental to provide a  
56  
57 204 baseline for future studies.

205

1  
2  
3  
4  
5  
6  
7  
8  
9  
10  
11  
12  
13  
14  
15  
16  
17  
18  
19  
20  
21  
22  
23  
24  
25  
26  
27  
28  
29  
30  
31  
32  
33  
34  
35  
36  
37  
38  
39  
40  
41  
42  
43  
44  
45  
46  
47  
48  
49  
50  
51  
52  
53  
54  
55  
56  
57  
58  
59  
60  
61  
62  
63  
64  
65

206 2.2. Data collection on <sup>137</sup>Cs in reference soil sites of South America

207  
208 A literature survey was carried out using Web of Science databases on March 1, 2020. Most data were  
209 found in peer-reviewed scientific articles published in English and Portuguese languages (n=17),  
210 although inventories were also taken from unpublished PhD manuscripts (n=2). The search keywords  
211 ‘soil erosion’, ‘cesium-137’, ‘<sup>137</sup>Cs’ and ‘inventorie(s)’ were used in isolation and/or combination with  
212 additional keywords containing the country names of South America. In addition, six scientific articles  
213 that were not identified during the initial Web of Science search were included in the literature  
214 compilation during the review process. Three conditions were necessary to accept data: (1) the data  
215 were provided in Bq m<sup>-2</sup>, (2) sampling locations were provided or easy to obtain and (3) information  
216 about sampling procedures was detailed. The sampling year or the year of decay-correction were also  
217 required to standardise all the data compiled. Seven studies did not mention the sampling year or the  
218 year of decay-correction. In this case, we made the assumption that sampling was conducted 4 years  
219 before the report publication, corresponding to the mean duration between sampling and publication  
220 in the current literature survey. All the data was decay-corrected to 2020 according to Eq. (1)

$$^{137}\text{Cs}_{2020} (\text{Bq m}^{-2}) = ^{137}\text{Cs}_{\text{literature}} (\text{Bq m}^{-2}) e^{(-\lambda \cdot t)} \tag{1}$$

221  
222 where  $\lambda$  is the decay constant of <sup>137</sup>Cs ( $\lambda = \ln 2 / 30.2 \text{ y}$ ) and  $t$  is the time (year) since the sampling year  
223 as reported in the corresponding article or estimated following the above-mentioned method. Each  
224 entry in the database corresponds to one undisturbed soil profile for which the <sup>137</sup>Cs inventory has  
225 been calculated, its geographical coordinates (latitude, longitude, elevation), annual rainfall rates,  
226 sampling method, <sup>137</sup>Cs inventory and the associated standard deviation estimated by the author and  
227 the associated decay-corrected values calculated from Eq. (1). In total, a database of 103 <sup>137</sup>Cs  
228 inventories at reference soil sites has been compiled, in four different countries and one overseas

229 department of France (Antarctica = 2, Argentina = 10, Brazil = 38, Chile = 50, Uruguay = 2, French Guiana  
1  
2 230 = 1) between 5.3° North latitude and 62° South latitude and from 109.3° to 34.9° West longitude (Fig.  
3  
4 231 1). Mean annual precipitation, the year of decay-correction, altitude and standard deviation were  
5  
6  
7 232 reported for 98, 82, 71 and 40 <sup>137</sup>Cs inventories calculated at these reference soil sites, respectively.  
8  
9 233 Four <sup>137</sup>Cs inventories from Easter Island (Pacific Ocean) and Antarctica were removed as they were  
10  
11 234 not obtained on the main South-American continent. Of note, four inventories obtained near the  
12  
13 235 Amazon River (0 and 1 Bq m<sup>-2</sup> respectively) and in Southern Brazil (5 and 90 Bq m<sup>-2</sup>), analysed by Handl  
14  
15 236 et al. (2008) may have been sampled in erosional areas rather than at reference sites, which may have  
16  
17 237 an impact on the results of the current research. Conversely, the highest <sup>137</sup>Cs inventories were found  
18  
19 238 in the central part of Chile (3113 and 2860 Bq m<sup>-2</sup>), at 40° South latitude (Schuller et al., 2002). These  
20  
21 239 inventories, with elevated <sup>137</sup>Cs concentrations, may have been sampled in accumulation areas instead  
22  
23 240 of reference locations. These six samples were considered as anomalous.  
24  
25  
26  
27  
28  
29 241 To gain insight into the accuracy of the baseline map of <sup>137</sup>Cs fallout derived from this dataset,  
30  
31 242 additional unpublished <sup>137</sup>Cs inventories in undisturbed soil profiles were used in the present study. In  
32  
33 243 total, 24 soil cores were collected by co-authors in Uruguay down to a soil depth of 20cm to  
34  
35 244 characterize three reference sites. All soil samples were collected using an Eijkelkamp soil sampler (5  
36  
37 245 cm diameter) and then stored in polyethylene bags. Samples were ground and passed through a 2 mm  
38  
39 246 sieve, then placed in 250 mL plastic Marinelli beakers. Gamma-ray measurements of <sup>137</sup>Cs (662 keV)  
40  
41 247 were obtained by high purity germanium detector (HPGe) (Canberra) at Laboratorio de Radioquímica  
42  
43 248 (Centro de Investigaciones Nucleares, Universidad de la República, Montevideo, Uruguay) and at  
44  
45 249 Laboratoire des Sciences du Climat et de l'Environnement (LSCE, Gif-sur-Yvette, France). In summary,  
46  
47  
48 250 among the 103 <sup>137</sup>Cs inventories compiled in the literature and the additional three <sup>137</sup>Cs inventories  
49  
50 251 collected by the co-authors, 96 <sup>137</sup>Cs inventories (Table 1) were used to perform the statistical analysis  
51  
52  
53 252 presented below.  
54  
55  
56  
57  
58 253

254 2.3. Spatial distribution of <sup>137</sup>Cs inventories in South America

255

256 According to the current literature review, the highest <sup>137</sup>Cs inventories in reference soil sites were  
257 found in the latitude band between 40 to 50° South (Fig. 2). From this location, inventories decreased  
258 towards both the Equator and Southern Patagonia, where the mean <sup>137</sup>Cs inventories were 97 and 279  
259 Bq m<sup>-2</sup>, respectively. The distribution of <sup>137</sup>Cs inventories in reference soil sites of South America is  
260 highly latitude-dependent, with a maximum in the 30-50° South latitude band, which is slightly higher  
261 than that proposed by UNSCEAR for that same latitude range. In contrast, the <sup>137</sup>Cs inventories in the  
262 0-20° South latitude band found in the literature is slightly lower than that proposed by UNSCEAR (Fig.  
263 3). Attention should be paid as published inventories were not found in the literature for the North-  
264 Western part of South America. Accordingly, the distribution determined from <sup>137</sup>Cs inventories in  
265 undisturbed soil profiles is mostly valid for Brazil, Uruguay, Argentina and Chile.

266 The typical pattern of <sup>137</sup>Cs deposition with latitude can be explained by the preferential exchange of  
267 air between the stratosphere and troposphere at mid-latitudes, as well as the air circulation patterns  
268 in the troposphere that both lead to an increased deposition of fallout radionuclides in the temperate  
269 regions and to a decreased deposition in the equatorial and polar regions (UNSCEAR, 2000). Indeed,  
270 the upward circulation that occurs in the equatorial region, known as Hadley circulation, is  
271 characterised by air masses rising from the ground into higher regions of the troposphere (Martin and  
272 McBride, 2012). According to UNSCEAR, this particular circulation pattern may explain the lower <sup>137</sup>Cs  
273 inventories in reference soil sites analysed in this latitude band, despite high annual rainfall rates  
274 reported in the Amazonian region (Handl et al., 2008). In contrast, <sup>137</sup>Cs inventories in reference soil  
275 sites are higher despite lower annual rainfall rates between 30 to 50° South latitude as a consequence  
276 of the Ferrel circulation, where air masses fall back down in the vicinity of the mid-latitudes, leading to  
277 an increase of radionuclide deposition in this part of South America (UNSCEAR, 2000).

278 A significant linear relationship was found between  $^{137}\text{Cs}$  inventories in reference soil sites and annual  
1  
2 279 rainfall rates provided by the authors ( $R^2=0.43$ ,  $n=92$ ,  $p < 0.001$ ). However, a wide dispersion of  $^{137}\text{Cs}$   
3  
4 280 inventories values is found for similar levels of precipitation (Fig. 4). In contrast, when reorganising the  
5  
6  
7 281 data according to the climatic circulation cells in which they are located, a significant relationship is  
8  
9 282 observed between mean annual rainfall rates and  $^{137}\text{Cs}$  inventories in soils of Argentina and Chile  
10  
11 283 ( $R^2=0.72$ ,  $n=54$ ,  $p < 0.001$ ). Furthermore, another linear relationship, although less significant, is found  
12  
13 284 for those reference soil sites located between the Equator and mid-latitudes ( $R^2=0.39$ ,  $n=38$ ,  $p < 0.001$ ).  
14  
15  
16  
17 285 Contrary to what has been observed for precipitation, no significant relationship was found between  
18  
19 286 the altitude reported by the authors at the reference sites and the  $^{137}\text{Cs}$  inventories ( $n=74$ ). However,  
20  
21  
22 287 when the analysis is performed for  $^{137}\text{Cs}$  inventories in reference soil sites located at the same latitude  
23  
24 288 although at a different altitude, it can be observed that  $^{137}\text{Cs}$  inventories tends to increase with the  
25  
26 289 altitude (data not shown). This observation confirms that made by Handl et al. (2008) who stated that  
27  
28  
29 290 maximum values were observed in regions of high altitude between  $23^\circ$  and  $29^\circ$  South latitude. In Chile,  
30  
31 291 Schuller et al. (2002) found a similar relationship for reference soil sites located in the central part of  
32  
33 292 the country, with higher values in elevated altitude areas, which are also exposed to higher rainfall.  
34  
35  
36 293 Furthermore, a low correlation is observed between the altitude of the sampling sites and the  $^{137}\text{Cs}$   
37  
38 294 inventories in reference sites located between the mid-latitudes and Southern Chile ( $R^2 = 0.20$ ,  $n=52$ ,  
39  
40  
41 295  $p < 0.01$ ). A step wise multiple regression indicated a significant relationship between observed and  
42  
43 296 predicted  $^{137}\text{Cs}$  inventories with a model including geographical information and annual rainfall rates  
44  
45 297 ( $R^2 = 0.74$ ,  $n = 71$ ,  $p < 0.001$ ) (Fig. 5).

46  
47  
48  
49 298

### 50 51 52 299 **3. Mapping $^{137}\text{Cs}$ initial fallout in South American soils**

#### 53 300 54 301 55 56 302 **3.1. Context**

57  
58 303

59 304

305 To the best of our knowledge, only very few studies (n= 7) were conducted to map bomb-derived <sup>137</sup>Cs  
306 fallout (Table 2). The spatial distribution of <sup>137</sup>Cs deposition was assessed when results of global fallout  
307 long-term monitoring programmes were available during the nuclear weapon tests period. By means  
308 of a GIS-based approach, Wright et al. (1999) used <sup>137</sup>Cs deposition data from the Arctic Monitoring and  
309 Assessment Programme (AMAP) with annual rainfall rates for the period 1955-1985 to predict <sup>137</sup>Cs  
310 deposition at the scale of the Arctic. Similarly, Pálsson et al. (2006) used activity concentrations of  
311 global fallout in precipitation at Rjúpnahæð, in addition to <sup>137</sup>Cs measurements in undisturbed soil  
312 profiles, to predict the spatial variation in global fallout of <sup>137</sup>Cs in Iceland. In Australia, Chappell et al.  
313 (2011a) used indicator co-simulation between 141 inventories in reference soil sites and gridded mean  
314 annual rainfall (1954–1990) to create a baseline map of <sup>137</sup>Cs fallout for Australian soils. More recently,  
315 Meusburger et al. (2020) used a digital soil mapping approach (McBratney et al., 2003) to predict the  
316 proportions and sources of artificial radionuclides in soils of several countries of Western Europe  
317 (France, Belgium, Switzerland, Southern Germany and Northern Italy). Their approach used a  
318 generalized additive models (GAM) with environmental factors.

319

### 320 3.2. Digital mapping of <sup>137</sup>Cs fallout in soils of South America

321  
322  
323 Mapping in the current research is based on a digital soil mapping (DSM) approach where field  
324 observations are combined with environmental data (covariates) and a statistical model to map the  
325 <sup>137</sup>Cs inventories at the scale of South America. Once a model is fitted to the data, it can be used to  
326 spatially predict the soil attribute at unobserved locations based on the observed environmental data  
327 at these locations. Environmental data should represent influential factors that explain the spatial  
328 variation of the target soil attribute. As previously mentioned, <sup>137</sup>Cs inventories in reference soil sites  
329 are strongly correlated with rainfall and latitude. We therefore retained two types of covariates : a  
330 spatially interpolated monthly rainfall database (WorldClim, <https://www.worldclim.org/>) at a

331 resolution of 30-arc seconds, calculated from the 1950-2000 period (Hijmans et al., 2005), and the  
1  
2 332 spatial coordinates (X and Y in meters).  
3  
4

5 333 Based on a cross validation procedure, a partial least square regression (PLSR) approach was selected.  
6

7 334 The theory underlying PLSR has been described in several statistical textbooks and articles  
8

9  
10 335 (Höskuldsson, 1988; Tenenhaus, 1998). PLSR could be deemed as a generalization of the multiple linear  
11

12 336 regression (Gerlach et al., 1979). PLSR is of particular interest because, unlike multiple linear  
13

14  
15 337 regression, it can analyze noisy data with numerous collinear variables.  
16

17  
18 338 The statistical analyses as well as the DSM procedures described in this section were carried out with  
19

20 339 the R software (Team R Core, 2013) and the following packages: caret (Kuhn, 2008), sf (Pebesma,  
21

22 340 2018), ithir (Malone, 2015), ggplot2 (Wickham, 2016), raster (Hijmans et al., 2015), corrplot (Wei et al.,  
23

24  
25 341 2017) and clhs (Roudier, 2011).  
26

27 342  
28  
29

30 343 Figure 6 shows the correlogram plot and the associated coefficients of correlation. The highest  
31

32 344 correlation was found between <sup>137</sup>Cs inventories and average monthly rainfall in August and  
33

34  
35 345 September ( $r=0.7$ ,  $p < 0.001$ ), followed by average monthly rainfall in May, June, July and average  
36

37 346 annual rainfall ( $r=0.6$ ,  $p < 0.001$ ), longitude ( $r=0.4$ ,  $p < 0.001$ ) and latitude ( $r=0.3$ ,  $p < 0.01$ ). Of note, no  
38

39  
40 347 correlation was observed for elevation. Based on this preliminary statistical analysis, seven covariates  
41

42 348 (latitude, longitude, average monthly rainfall in June, July, August, September and mean annual rainfall  
43

44 349 rates) were selected to perform the PLSR.  
45  
46

47  
48 350 Following the cross validation procedure, we showed that our quantitative model explained 46% of  
49

50 351 the <sup>137</sup>Cs variability observed and tended to underestimate inventories  $> 800 \text{ Bq m}^{-2}$ . The predicted  
51

52 352 <sup>137</sup>Cs inventories followed a right-skewed statistical distribution, with an average of  $348 \text{ Bq m}^{-2}$  and a  
53

54  
55 353 standard deviation of  $237 \text{ Bq m}^{-2}$ . Highest values (between  $1501$  to  $2057 \text{ Bq m}^{-2}$ ) were found in  
56

57 354 Colombia and few areas of the Andean Cordillera, while the vast majority of <sup>137</sup>Cs inventories lower  
58

59 355 than  $100 \text{ Bq m}^{-2}$  were found in the North-Eastern part of Brazil (Fig. 7). Surprisingly, high <sup>137</sup>Cs  
60  
61  
62  
63  
64  
65

1 356 inventories are predicted for countries located near the equator, where fallout should be the lowest  
2 357 according to UNSCEAR (2000). Of note, the highest inventories are mainly located along the Andean  
3  
4 358 Cordillera at high altitudes. Taking into account that the model does not include elevation as a  
5  
6  
7 359 covariable, the deposition pattern of <sup>137</sup>Cs is closely linked to that of rainfall rates and it may reflect  
8  
9 360 the orographic effects that occur in mountainous environments. However, these mountainous areas  
10  
11 361 predominantly consist of rock outcrops and bare soil surfaces. Consequently, areas above 1,800 m a.s.l  
12  
13 362 have been masked using the GMTED2010 30-arc-second elevation database (Danielson and Gesch,  
14  
15  
16 363 2011). As previously mentioned, most of the <sup>137</sup>Cs inventories in undisturbed soil profiles used to  
17  
18 364 develop the digital soil mapping approach were measured in the eastern part of South America and in  
19  
20  
21 365 Southern Chile. The estimates provided for the other regions (i.e. northern and western parts of the  
22  
23 366 subcontinent) should therefore be interpreted with caution. Additional sampling in these areas will be  
24  
25  
26 367 necessary to improve model predictions of <sup>137</sup>Cs global fallout in South America.

27  
28  
29 368 The baseline map of <sup>137</sup>Cs inventories in reference soil sites (Bq m<sup>-2</sup>, 2020) with a spatial resolution of  
30  
31 369 2 km (projection: WGS 84 - World Geodetic System 1984) was compiled using ESRI ArcGIS 10.6  
32  
33 370 Desktop. The validity of the proposed approach to predict the spatial distribution of the reference  
34  
35  
36 371 levels of fallout <sup>137</sup>Cs at the subcontinental-scale of South America relies on the assumption that studies  
37  
38 372 listed in our database followed the recommendations to select and sample undisturbed soil sites. Since  
39  
40  
41 373 the coefficient of variation of multiple samples collected to characterize one reference site is not  
42  
43 374 always reported by authors, the observations uncertainties are difficult to quantify. As reported in the  
44  
45 375 literature, <sup>137</sup>Cs inventories in reference soil sites have a coefficient of variation of approximately 20%,  
46  
47  
48 376 as a consequence of random and systematic spatial variability, sampling variability and measurement  
49  
50 377 precisions (Loughran et al., 2002; Owens and Walling, 1996; Pennock, 2000). Accordingly, the map  
51  
52 378 predictions provided in this study for each grid should be interpreted as a trend rather than a single  
53  
54  
55 379 accurate value.

56  
57 380  
58  
59  
60  
61  
62  
63  
64  
65

381 A non-parametric bootstrap approach was used to quantify the prediction uncertainties of the map  
1  
2 382 (Efron and Tibshirani, 1994; Liddicoat et al., 2015; Rossel et al., 2015). In this approach, data used for  
3  
4 383 model calibration was selected using random sampling with replacement, with sample size equal to 95  
5  
6  
7 384 % of the number of data in the available dataset. This calibration step is iterated 100 times leading to  
8  
9 385 100 contributing predictions at each prediction location. These predictions collectively constituted an  
10  
11 386 empirical probability distribution (EDP) of the  $^{137}\text{Cs}$  inventories. We computed the 95 % prediction  
12  
13 387 confidence interval by subtracting the 97.5% quantile to the 2.5 % quantile of the EDP. For clarity, the  
14  
15 388 coefficient of variation (in %) was computed by dividing the average prediction by the 95% confidence  
16  
17 389 interval (Fig. 8). For most part of South America, the relative error was comprised between 0 and 10  
18  
19 390 %. The highest uncertainties could be observed in two areas located in the North-Eastern part of Brazil  
20  
21 391 and along the Pacific coast of Peru, where the map predictions of  $^{137}\text{Cs}$  inventories in reference soil  
22  
23 392 sites are the lowest (0 to 100 Bq m<sup>-2</sup> in 2020).  
24  
25  
26  
27

28 393

29  
30 394

### 31 395 3.3. Improving spatial predictions through additional sampling

32  
33  
34  
35 396

36  
37 397 Sampling design plays an essential role in a digital soil mapping approach as it controls the estimation  
38  
39 398 of the statistical model parameters and also the spatial predictions. A sound sampling design is  
40  
41 399 expected to provide a scheme of representative samples covering the study area with a relatively small  
42  
43 400 sample size for financial and logistical reasons. If it is assumed that the soil property is linked to  
44  
45 401 environmental covariates, a robust strategy is to ensure that the measurements are also uniformly  
46  
47 402 spread in the feature (i.e. covariates) space. However, the collected data of the present study did not  
48  
49 403 follow any sampling design as they were compiled from various independent studies, leading to large  
50  
51 404 areas devoid of sampling observations or places with clusters. Accordingly, an experiment was  
52  
53 405 conducted to generate new sampling locations in order to fill the gap in feature space of the selected  
54  
55 406 environmental variables. This can be achieved using conditioned Latin Hypercube sampling (cLHS)  
56  
57  
58  
59  
60  
61  
62  
63  
64  
65

407 (Minasny and McBratney, 2006; Wadoux et al., 2019), which guarantees the full coverage of a  
408 multivariate feature space. We ran the algorithm with the selected covariates of our model to produce  
409 a set of 10 new sampling locations that should be analysed in priority in the future to improve the map  
410 in addition to the existing samples (Table 3) (Fig. 7).

#### 4. Potential for application of the $^{137}\text{Cs}$ technique in South America

416 In South America, where the input of bomb-derived  $^{137}\text{Cs}$  fallout has stopped since the 1980s,  $^{137}\text{Cs}$   
417 inventories in soils are continuously decreasing as a consequence of radioactive decay. One major  
418 challenge is to clearly identify areas where the  $^{137}\text{Cs}$  technique could be applied to address Earth  
419 Science research questions, or those where it will either become difficult or impossible. Of note, sites  
420 exposed to erosion in intensively cultivated catchments could be depleted in  $^{137}\text{Cs}$  which would  
421 therefore prevent the application of the  $^{137}\text{Cs}$  technique in these locations.

422 Chile is the country of South America where information about  $^{137}\text{Cs}$  inventories in reference soil sites  
423 is the most documented ( $n=48$ ), including two sites located on Easter Island in the Pacific Ocean). In  
424 the central part of Chile, extending from 36 to 42° South latitude, a mean  $^{137}\text{Cs}$  inventory of 563 Bq m<sup>-2</sup>  
425 can be calculated from 30 reference soil sites. The high content of  $^{137}\text{Cs}$  in soils allowed for the use of  
426 the  $^{137}\text{Cs}$  technique to quantify soil redistribution rates under different land uses and management  
427 practices (Schuller et al., 2003b). Of note, the standard deviation (SD) expressed in Bq m<sup>-2</sup> was  
428 mentioned for 14 reference soil sites (Banfield et al., 2018; Schuller et al., 2003a), while the SD was  
429 expressed in Bq kg<sup>-1</sup> without any information regarding the bulk density of soils sampled for calculating  
430 the other  $^{137}\text{Cs}$  inventories collected in the country (Schuller et al., 2002). Although  $^{137}\text{Cs}$  inventories  
431 are lower in the Patagonian part of Chile with a mean value of 280 Bq m<sup>-2</sup> ( $n=16$ ), the applicability of  
432 the  $^{137}\text{Cs}$  technique could be explored to investigate the soil response to environmental changes under  
433 colder climates (Navas et al., 2018).

434 In Argentina, <sup>137</sup>Cs soil profiles have been collected in the Pampa Ondulada region of Buenos Aires  
1  
2 435 Province (Bujan et al., 2003), in soils of La Plata region (Montes et al., 2013), in natural and semi-natural  
3  
4 436 grassland areas of San Luis Province (Ayub et al., 2008) and in the Patagonian Andean forests (La  
5  
6  
7 437 Manna et al., 2019). These studies showed that <sup>137</sup>Cs inventories were sufficient in these regions to  
8  
9 438 calculate soil redistribution rates based on this technique. Of note, there is a lack of <sup>137</sup>Cs inventory  
10  
11 439 data in the literature for the Argentinian provinces located between 25 to 40° South latitudes, where  
12  
13 440 inventories in reference soil sites should be the highest of South America according to UNSCEAR  
14  
15 441 (2000). Thus, the <sup>137</sup>Cs technique should be successfully implemented in this country exposed to  
16  
17 442 elevated levels of both water and wind erosion (Ares et al., 2016; Mendez and Buschiazzo, 2010).  
18  
19  
20  
21

22 443 In Uruguay, only two <sup>137</sup>Cs inventory had been documented so far in the literature (Alonso et al., 2012;  
23  
24 444 Tassano et al., 2020). Alonso et al. (2012) assessed soil erosion rates in a forested micro-catchment  
25  
26 445 occupied by eucalyptus plantations within the Río Negro River basin. The three additional <sup>137</sup>Cs  
27  
28 446 inventories collected in Uruguay by co-authors of the current research remained in the same order of  
29  
30 447 magnitude, with an average value of  $336 \pm 13 \text{ Bq m}^{-2}$ . These values are consistent with <sup>137</sup>Cs inventories  
31  
32 448 found in the neighbouring Rio Grande do Sul state, in southernmost Brazil, where <sup>137</sup>Cs inventories  
33  
34 449 followed an increasing gradient from the Uruguayan border in the South ( $315 \pm 22 \text{ Bq m}^{-2}$ ) to the North  
35  
36 450 ( $1022 \pm 292 \text{ Bq m}^{-2}$ ) (Didone et al., 2019; Handl et al., 2008; Minella et al., 2014).  
37  
38  
39  
40

41 451 In general, <sup>137</sup>Cs inventories measured in sites of Brazil located below 20°S are high enough to  
42  
43 452 reconstruct soil redistribution rates (Bacchi et al., 2000; Correchel et al., 2005; Didone et al., 2019;  
44  
45 453 Macêdo, 2009; Minella et al., 2014). In addition to these studies where the <sup>137</sup>Cs technique has been  
46  
47 454 used successfully, many regions in South America should have received enough fallout to reconstruct  
48  
49 455 soil redistribution rates (Fig 9.A). This includes most of the agricultural regions located in Paraguay and  
50  
51 456 Argentina between 20 to 45°S, as well as Mato Grosso state (Brazil) where intensification in agriculture-  
52  
53 457 forest frontiers is observed (Garrett et al., 2018) (Fig 9. B, C).  
54  
55  
56  
57  
58  
59  
60  
61  
62  
63  
64  
65

1  
2 458 Despite the high mean annual rainfall rates observed in the equatorial regions, low  $^{137}\text{Cs}$  inventories in  
3  
4 459 reference soil sites were observed in the range of latitudes comprised between 2°N and 10°S. As  
5  
6 460 previously mentioned, one reason that may explain this observation is the upward circulation of air  
7  
8 461 masses as a consequence of Hadley circulation in this latitude band. Soil erosion studies based on  $^{137}\text{Cs}$   
9  
10 462 inventories should be difficult to conduct in the North-Eastern part of Brazil. Furthermore, to the best  
11  
12 463 of our knowledge, no studies on  $^{137}\text{Cs}$  inventories in reference soil sites have been conducted in  
13  
14 464 Suriname, Guyana, Venezuela, Colombia and Peru.

15  
16  
17 465 One study investigating soil erosion in a mountainous watershed of Ecuador (2°S) with the  $^{137}\text{Cs}$   
18  
19 466 technique was not retained in the current review because geographical information of  $^{137}\text{Cs}$  inventories  
20  
21 467 in reference soil site was erroneous (Henry et al., 2013). In this study, no flat undisturbed sites that can  
22  
23 468 serve as typical reference sites were found, and reference sites were selected based on  $^{137}\text{Cs}$  activity  
24  
25 469 patterns with depth and land use history. A mean  $^{137}\text{Cs}$  reference value of  $2260 \pm 330 \text{ Bq m}^{-2}$  was  
26  
27 470 established with no decay-correction date presented. Although this value should be taken with  
28  
29 471 caution, it appears valuable to investigate  $^{137}\text{Cs}$  initial fallout in equatorial regions of South America.  
30  
31 472 Indeed, anomalous high values of  $^{137}\text{Cs}$  activities were also observed in surface soils of Venezuela  
32  
33 473 (LaBrecque et al., 2001) and one  $^{137}\text{Cs}$  inventory in a reference soil site of French Guiana (de Tombeur  
34  
35 474 et al., 2020) was found to be twice than what was expected from the UNSCEAR predictions for this  
36  
37 475 latitude band ( $1022 \pm 293$  compared to  $509 \pm 57 \text{ Bq m}^{-2}$ , decay-corrected to 2016).  
38  
39  
40  
41  
42

43 476

## 44 45 46 477 **5. Perspectives for future research**

47 478

48 479

49  
50  
51  
52 480 Beside the fact that baseline maps of  $^{137}\text{Cs}$  fallout are of fundamental importance in case of future  
53  
54 481 accidental radionuclide emissions, their use in geomorphological studies provides an opportunity to  
55  
56 482 reconstruct soil redistribution due to soil erosion processes at larger scales (Chappell et al., 2011b;  
57  
58 483 Meusburger et al., 2020). Although estimates of erosion rates at continental scales are debated (Fiener  
59  
60  
61  
62  
63  
64  
65

484 and Auerswald, 2016; Panagos et al., 2015; Panagos et al., 2016), prediction of  $^{137}\text{Cs}$  initial fallout at  
1  
2 485 kilometric scales offers the potential to increase our knowledge of soil erosion processes in catchments  
3  
4 486 through the use of the  $^{137}\text{Cs}$  inventory technique and its upscaling (Lizaga et al., 2018). In general, the  
5  
6  
7 487 spatial distribution of anthropogenic radionuclides in soils and their use as tracers of environmental  
8  
9 488 processes is of significant importance for Earth and atmospheric sciences (Bhandari, 1970; Everett et  
10  
11 489 al., 2008; Hirose, 2012; Igarashi et al., 2011; Jagercikova et al., 2017).

14 490  
15  
16 491 Considering that no radioactive fallout occurred since 1980 in South America, and as a consequence of  
17  
18 492 radioactive decay,  $^{137}\text{Cs}$  activities in soils of South America will continue decreasing and become  
19  
20  
21 493 increasingly difficult to measure without ultra-low background gamma spectrometry facilities (Evrard  
22  
23 494 et al., 2020). The development of surrogate tracers appears necessary for further geomorphological  
24  
25 495 studies using fallout radionuclides, especially in the Southern hemisphere that received only 23% of  
26  
27  
28 496 the total bomb-fallout emitted worldwide according to UNSCEAR (2000). In the last several decades,  
29  
30 497 the efficiency of the  $^{239+240}\text{Pu}$  inventory technique to quantify soil erosion rates has been demonstrated  
31  
32  
33 498 in countries located in the Northern hemisphere (Alewell et al., 2014; Alewell et al., 2017; Meusbürger  
34  
35 499 et al., 2016). To the best of our knowledge, one study investigating soil erosion rates using  $^{239}\text{Pu}$  was  
36  
37  
38 500 carried out in Australia (Lal et al., 2020). In contrast to  $^{137}\text{Cs}$  and  $^{239+240}\text{Pu}$ , the continuous input of fallout  
39  
40 501 radionuclides including excess lead-210 ( $^{210}\text{Pb}_{\text{xs}}$ ) should be considered as an efficient tracer of soil  
41  
42 502 erosion, especially in regions where low  $^{137}\text{Cs}$  fallout occurred (Evrard et al., 2020; Gaspar et al., 2013;  
43  
44  
45 503 Porto et al., 2009; Walling et al., 2011). The effectiveness of these techniques in South America remains  
46  
47 504 unknown and it should be investigated to assess soil redistribution under climate and land use changes.

50 505  
51  
52  
53 506 Overall, a significant lack of information about  $^{137}\text{Cs}$  inventories in reference soil sites is observed in  
54  
55 507 areas of South America exposed to extensive clearcutting, overgrazing and cropping intensification. As  
56  
57  
58 508 an example, central Brazil in general and the Cerrado Biome in particular (Fig. 9) should have received

509 sufficient levels of  $^{137}\text{Cs}$  fallout to investigate soil redistribution rates induced by deforestation and  
1  
2 510 land uses changes. A better characterization of  $^{137}\text{Cs}$  fallout at the scale of South America is also  
3  
4 511 required with the addition of soil inventory measurements in North-Western parts of South America,  
5  
6  
7 512 where some areas should have received sufficient fallout to conduct geomorphological studies despite  
8  
9 513 what was previously expected from the UNSCEAR reports. Accordingly, future research should strive  
10  
11 514 to ensure that basic information (e.g. rainfall databases used) and details on the sampling design (e.g.  
12  
13 515 number of soil profiles used to estimate  $^{137}\text{Cs}$  inventories in reference soil sites) are properly  
14  
15 516 documented to improve future model predictions and better consider the issues of uncertainty and  
16  
17  
18 517 data reliability.  
19  
20  
21

22 518

## 24 519 **6. Conclusions**

25 520

26 521

27  
28  
29 522 Based on a compilation of published information, additional measurements and rainfall data over the  
30  
31 523 period 1950-2000, this work represents one of the first approaches to spatialize the reference levels  
32  
33 524 of fallout  $^{137}\text{Cs}$  at the subcontinental-scale of South America. The current research demonstrates that  
34  
35 525 the  $^{137}\text{Cs}$  inventories technique should be appropriate to assess soil redistribution rates during the  
36  
37 526 agricultural intensification period in Chile, Argentina, Uruguay and Southern Brazil where detectable  
38  
39 527 levels of  $^{137}\text{Cs}$  can be expected to be found in sites exposed to erosion. This technique should  
40  
41 528 theoretically be applicable in other countries where no information was available to date, such as  
42  
43 529 Paraguay, Bolivia and Peru. Further investigations should be conducted in equatorial regions where  
44  
45 530 information on  $^{137}\text{Cs}$  fallout is scarce. Our results indicate that  $^{137}\text{Cs}$  inventories in this region may be  
46  
47 531 higher than expected from the UNSCEAR reports. Additional sampling is necessary to verify whether it  
48  
49 532 will be either complicated or impossible to quantify soil erosion using bomb-derived  $^{137}\text{Cs}$  in equatorial  
50  
51 533 regions exposed to extensive clearcutting and agricultural expansion.  
52  
53  
54  
55  
56

57  
58 534 In addition to the priority complementary sampling locations identified through the use of conditioned  
59  
60  
61  
62  
63  
64  
65

1  
2 536 Latin Hypercube sampling (cLHS), the South American continent could be subdivided into regions  
3  
4 537 corresponding to different biomes in which the fate of the global <sup>137</sup>Cs fallout is expected to be  
5  
6 538 homogeneous. Consequently, future sampling campaigns should strive to ensure that all biomes are  
7  
8 well covered with a sufficient number of soil profiles.

9 539 The map generated can be used both to validate <sup>137</sup>Cs inventories collected in the field or as a decision-  
10  
11 540 support tool to guide the implementation of the <sup>137</sup>Cs technique in intensive agricultural landscapes of  
12  
13 541 South America. This baseline map will also be particularly useful for a wide range of Earth science  
14  
15 542 applications, including the vertical transfers in soils, the circulation of air masses and ocean currents.  
16  
17 543 Of note, this map is provisional as it is only based on the data published until early 2020 and it can be  
18  
19 544 optimized through the incorporation of additional <sup>137</sup>Cs inventory measurements in South America.  
20  
21  
22  
23  
24  
25  
26  
27  
28

29 545

30 546

## 31 **Acknowledgements**

32 548 Pierre-Alexis Chaboche received a PhD fellowship from the University of Versailles-Saint-Quentin (a  
33  
34 549 founding member of University Paris-Saclay). The initiation of this collaboration between France and  
35  
36 550 Brazil was supported by a grant from CAPES-COFECUB (project Te870-15), and the CAPES-PRINT  
37  
38 551 programme. Collaboration between France and Uruguay is supported by an applied research project  
39  
40 552 from the Fondo Maria Viñas (FMV\_1\_2019\_1\_156244) funded by the National Agency of Research and  
41  
42 553 Innovation (ANII, Uruguay).  
43  
44  
45  
46

## 47 **7. References**

48 554  
49 555  
50  
51 556 Alewell, C., Meusburger, K., Juretzko, G., Mabit, L. and Ketterer, M.E., 2014. Suitability of <sup>239+240</sup>Pu  
52 557 and <sup>137</sup>Cs as tracers for soil erosion assessment in mountain grasslands. *Chemosphere*, 103:  
53 558 274-280.  
54 559 Alewell, C., Pitois, A., Meusburger, K., Ketterer, M. and Mabit, L., 2017. <sup>239+240</sup>Pu from  
55 560 “contaminant” to soil erosion tracer: Where do we stand? *Earth-Science Reviews*, 172: 107-  
56 561 123.  
57 562 Almgren, S., Nilsson, E., Erlandsson, B. and Isaksson, M., 2006. GIS supported calculations of <sup>137</sup>Cs  
58 563 deposition in Sweden based on precipitation data. *Science of the Total Environment*, 368(2-  
59 564 3): 804-813.  
60  
61  
62  
63  
64  
65

565 Alonso, J., Audicio, P., Martinez, L., Scavone, M. and Rezzano, E., 2012. Comparison of measured  
1 566 <sup>137</sup>Cs data and USLE/RUSLE simulated long-term erosion rates. *Agrociencia-Sitio en*  
2 567 *Reparación*, 16(3): 261-267.

3 568 Aoyama, M., Hirose, K. and Igarashi, Y., 2006. Re-construction and updating our understanding on  
4 569 the global weapons tests <sup>137</sup>Cs fallout. *Journal of Environmental Monitoring*, 8(4): 431.

5 570 Ares, M.G., Bongiorno, F., Holzman, M., Chagas, C., Varni, M. and Entraigas, I., 2016. Water erosion  
6 571 and connectivity analysis during a year with high precipitations in a watershed of Argentina.  
7 572 *Hydrology Research*, 47(6): 1239-1252.

8 573 Ayub, J.J., Velasco, R., Rizzotto, M., Quintana, E. and Aguiar, J., 2008. <sup>40</sup>K, <sup>115</sup>Cs and <sup>226</sup>Ra Soil and  
9 574 Plant Content in Seminatural Grasslands of Central Argentina, AIP Conference Proceedings.  
10 575 AIP, pp. 273-276.

11 576 Bacchi, O.O.S., Reichard, K., Sparovek, G. and Ranieri, S.B.L., 2000. Soil erosion evaluation in a small  
12 577 watershed in Brazil through <sup>137</sup>Cs fallout redistribution analysis and conventional models.  
13 578 *Acta Geologica Hispanica*, 35(3-4): 251-259.

14 579 Bakker, M.M., Govers, G., Jones, R.A. and Rounsevell, M.D.A., 2007. The Effect of Soil Erosion on  
15 580 Europe's Crop Yields. *Ecosystems*, 10(7): 1209-1219.

16 581 Bakker, M.M., Govers, G. and Rounsevell, M.D., 2004. The crop productivity–erosion relationship: an  
17 582 analysis based on experimental work. *Catena*, 57(1): 55-76.

18 583 Banfield, C.C., Braun, A.C., Barra, R., Castillo, A. and Vogt, J., 2018. Erosion proxies in an exotic tree  
19 584 plantation question the appropriate land use in Central Chile. *CATENA*, 161: 77-84.

20 585 Becker, A.G., Moraes, B.S., Menezes, C.C., Loro, V.L., Santos, D.R., Reichert, J.M. and Baldisserotto, B.,  
21 586 2009. Pesticide contamination of water alters the metabolism of juvenile silver catfish,  
22 587 *Rhamdia quelen*. *Ecotoxicol Environ Saf*, 72(6): 1734-9.

23 588 Bennett, B.G., 2002. Worldwide dispersion and deposition of radionuclides produced in atmospheric  
24 589 tests : Fallout from atmospheric nuclear tests : Impact on science and society. *Health Physics*,  
25 590 82(5): 644-655.

26 591 Bhandari, N., 1970. Transport of air in the stratosphere as revealed by radioactive tracers. *Journal of*  
27 592 *Geophysical Research*, 75(15): 2927-2930.

28 593 Bouisset, P., Nohl, M., Bouville, A. and Leclerc, G., 2018. Inventory and vertical distribution of <sup>137</sup>Cs,  
29 594 <sup>239+240</sup>Pu and <sup>238</sup>Pu in soil from Raivavae and Hiva Oa, two French Polynesian islands in the  
30 595 southern hemisphere. *Journal of Environmental Radioactivity*, 183: 82-93.

31 596 Buesseler, K.O. and Benitez, C.R., 1994. Determination of mass accumulation rates and sediment  
32 597 radionuclide inventories in the deep Black Sea. *Deep-Sea Research Part I-Oceanographic*  
33 598 *Research Papers*, 41(11-12): 1605-1615.

34 599 Bujan, A., Santanatoglia, O.J., Chagas, C., Massobrio, M., Castiglioni, M., Yanez, M., Ciallella, H. and  
35 600 Fernandez, J., 2003. Soil erosion evaluation in a small basin through the use of Cs-137  
36 601 technique. *Soil & Tillage Research*, 69(1-2): 127-137.

37 602 Camargo, F.A.O., Silva, L.S., Merten, G.H., Carlos, F.S., Baveye, P.C. and Triplett, E.W., 2017. Brazilian  
38 603 Agriculture in Perspective. *Advances in Agronomy*, pp. 53-114.

39 604 Cambray, R., Playford, K., Lewis, G. and Carpenter, R., 1989. Radioactive fallout in air and rain: results  
40 605 to the end of 1988. AERE R13575. Atomic Energy Authority, London, UK.

41 606 Chappell, A., Hancock, G., Viscarra Rossel, R.A. and Loughran, R., 2011a. Spatial uncertainty of  
42 607 the <sup>137</sup>Cs reference inventory for Australian soil. *Journal of Geophysical Research*, 116(F4).

43 608 Chappell, A., Viscarra Rossel, R.A. and Loughran, R., 2011b. Spatial uncertainty of <sup>137</sup>Cs-derived net  
44 609 (1950s–1990) soil redistribution for Australia. *Journal of Geophysical Research: Earth Surface*,  
45 610 116(F4).

46 611 Chartin, C., Evrard, O., Salvador-Blanes, S., Hirschberger, F., Van Oost, K., Lefèvre, I., Daroussin, J. and  
47 612 Macaire, J.-J., 2013. Quantifying and modelling the impact of land consolidation and field  
48 613 borders on soil redistribution in agricultural landscapes (1954–2009). *Catena*, 110: 184-195.

49 614 Correchel, V., Bacchi, O.O.S., Reichardt, K. and De Maria, I.C., 2005. Random and systematic spatial  
50 615 variability of <sup>137</sup>Cs inventories at reference sites in South-Central Brazil. *Scientia Agricola*,  
51 616 62(2): 173-178.

617 de Tombeur, F., Cornu, S., Bourlès, D., Duvivier, A., Pupier, J., Aster, T., Brossard, M. and Evrard, O.,  
1 618 2020. Retention of  $^{10}\text{Be}$ ,  $^{137}\text{Cs}$  and  $^{210}\text{Pb}$ s in soils: Impact of physico-chemical  
2 619 characteristics. *Geoderma*, 367.

3 620 Didone, E.J., Minella, J.P.G., Schneider, F.J.A., Londero, A.L., Lefevre, I. and Evrard, O., 2019.  
4 621 Quantifying the impact of no-tillage on soil redistribution in a cultivated catchment of  
5 622 Southern Brazil (1964-2016) with Cs-137 inventory measurements. *Agriculture Ecosystems &*  
6 623 *Environment*, 284.

8 624 Efron, B. and Tibshirani, R.J., 1994. An introduction to the bootstrap. CRC press.

9 625 Ehhalt, D., 1973. Turnover times of  $^{137}\text{Cs}$  and HTO in the troposphere and removal rates of natural  
10 626 aerosol particles and water vapor. *Journal of Geophysical Research*, 78(30): 7076-7086.

11 627 Everett, S., Tims, S., Hancock, G., Bartley, R. and Fifield, L.K., 2008. Comparison of Pu and  $^{137}\text{Cs}$  as  
12 628 tracers of soil and sediment transport in a terrestrial environment. *Journal of Environmental*  
13 629 *Radioactivity*, 99(2): 383-393.

15 630 Evrard, O., Bielders, C.L., Vandaele, K. and van Wesemael, B., 2007. Spatial and temporal variation of  
16 631 muddy floods in central Belgium, off-site impacts and potential control measures. *Catena*,  
17 632 70(3): 443-454.

19 633 Evrard, O., Chaboche, P.-A., Ramon, R., Foucher, A. and Lacey, J.P., 2020. A global review of  
20 634 sediment source fingerprinting research incorporating fallout radiocesium ( $^{137}\text{Cs}$ ).  
21 635 *Geomorphology*: 107103.

22 636 FAO, 2015. Status of the world's soil resources: main report. FAO : ITPS, Rome.

23 637 FAO/IAEA, 2017. Use of  $^{137}\text{Cs}$  for soil erosion assessment. Fulajtar, E., Mabit, L., Renschler, C.S., Lee  
24 638 Zhi Yi, A., . In: F.a.A.O.o.t.U. Nations (Editor), Rome, Italy, pp. 64.

26 639 Fiener, P. and Auerwald, K., 2016. Comment on "The new assessment of soil loss by water erosion in  
27 640 Europe" by Panagos et al. (*Environmental Science & Policy* 54 (2015) 438–447).  
28 641 *Environmental Science & Policy*, 57: 140-142.

29 642 Foucher, A., Salvador-Blanes, S., Evrard, O., Simonneau, A., Chapron, E., Courp, T., Cerdan, O.,  
30 643 Lefèvre, I., Adriaensen, H., Lecompte, F. and Desmet, M., 2014. Increase in soil erosion after  
31 644 agricultural intensification: Evidence from a lowland basin in France. *Anthropocene*, 7: 30-41.

33 645 Fukuyama, T., Takenaka, C. and Onda, Y., 2005.  $^{137}\text{Cs}$  loss via soil erosion from a mountainous  
34 646 headwater catchment in central Japan. *Science of the total environment*, 350(1-3): 238-247.

35 647 Furuichi, T. and Wasson, R.J., 2013. Caesium-137 in Southeast Asia: Is there enough left for soil  
36 648 erosion and sediment redistribution studies? *Journal of Asian Earth Sciences*, 77: 108-116.

38 649 Garcia Agudo, E., 1998. Global distribution of Cs-137 inputs for soil erosion and sedimentation  
39 650 studies, In: *Use of Caesium-137 in the Study of Soil Erosion and Sedimentation*. IAEA TECDOC  
40 651 1028., pp. 117-121.

41 652 Garrett, R.D., Koh, I., Lambin, E.F., De Waroux, Y.I.P., Kastens, J.H. and Brown, J., 2018. Intensification  
42 653 in agriculture-forest frontiers: Land use responses to development and conservation policies  
43 654 in Brazil. *Global Environmental Change*, 53: 233-243.

45 655 Gaspar, L., Navas, A., Walling, D., Machín, J. and Arozamena, J.G., 2013. Using  $^{137}\text{Cs}$  and  $^{210}\text{Pb}$  to  
46 656 assess soil redistribution on slopes at different temporal scales. *Catena*, 102: 46-54.

47 657 Gerlach, R.W., Kowalski, B.R. and Wold, H.O., 1979. Partial least squares path modelling with latent  
48 658 variables, WASHINGTON UNIV SEATTLE LAB FOR CHEMOMETRICS.

49 659 Gilbert, E.S., Land, C.E. and Simon, S.L., 2002. Health effects from fallout. *Health Physics*, 82(5): 726-  
50 660 735.

52 661 Handl, J., Sachse, R., Jakob, D., Michel, R., Evangelista, H., Gonçalves, A.C. and de Freitas, A.C., 2008.  
53 662 Accumulation of  $^{137}\text{Cs}$  in Brazilian soils and its transfer to plants under different climatic  
54 663 conditions. *Journal of Environmental Radioactivity*, 99(2): 271-287.

55 664 Health and Safety Laboratory, E., New York 10014, 1977. Final tabulation of monthly strontium-90  
56 665 fallout data : 1954-1976.

58 666 Henry, A., Mabit, L., Jaramillo, R.E., Cartagena, Y. and Lynch, J.P., 2013. Land use effects on erosion  
59 667 and carbon storage of the Rio Chimbo watershed, Ecuador. *Plant and Soil*, 367(1-2): 477-491.

668 Hijmans, R.J., Cameron, S.E., Parra, J.L., Jones, P.G. and Jarvis, A., 2005. Very high resolution  
1 669 interpolated climate surfaces for global land areas. *International Journal of Climatology*,  
2 670 25(15): 1965-1978.

3 671 Hijmans, R.J., Van Etten, J., Cheng, J., Mattiuzzi, M., Sumner, M., Greenberg, J.A., Lamigueiro, O.P.,  
4 672 Bevan, A., Racine, E.B. and Shortridge, A., 2015. Package 'raster'. R package, 734.

5 673 Hirose, K., 2012. Uranium, thorium and anthropogenic radionuclides as atmospheric tracers,  
6 674 *Handbook of Environmental Isotope Geochemistry*. Springer, pp. 591-611.

7 675 Höskuldsson, A., 1988. PLS regression methods. *Journal of chemometrics*, 2(3): 211-228.

8 676 Igarashi, Y., Fujiwara, H. and Jugder, D., 2011. Change of the Asian dust source region deduced from  
9 677 the composition of anthropogenic radionuclides in surface soil in Mongolia. *Atmospheric  
10 678 Chemistry and Physics*, 11(14): 7069.

11 679 Jagercikova, M., Cornu, S., Bourlès, D., Evrard, O., Hatté, C. and Balesdent, J., 2017. Quantification of  
12 680 vertical solid matter transfers in soils during pedogenesis by a multi-tracer approach. *Journal  
13 681 of Soils and Sediments*, 17(2): 408-422.

14 682 Keesstra, S.D., Bouma, J., Wallinga, J., Tittonell, P., Smith, P., Cerdà, A., Montanarella, L., Quinton,  
15 683 J.N., Pachepsky, Y., van der Putten, W.H., Bardgett, R.D., Moolenaar, S., Mol, G., Jansen, B.  
16 684 and Fresco, L.O., 2016. The significance of soils and soil science towards realization of the  
17 685 United Nations Sustainable Development Goals. *Soil*, 2(2): 111-128.

18 686 Kuhn, M., 2008. Building predictive models in R using the caret package. *Journal of statistical  
19 687 software*, 28(5): 1-26.

20 688 La Manna, L., Gaspar, L., Tarabini, M., Quijano, L. and Navas, A., 2019. Cs-137 inventories along a  
21 689 climatic gradient in volcanic soils of Patagonia: Potential use for assessing medium term  
22 690 erosion processes. *Catena*, 181.

23 691 LaBrecque, J., Rosales, P. and Cordoves, P., 2001. Anomalously high values of cesium-137 in soils on  
24 692 the Peninsula de Paraguana (Venezuela). *Journal of Radioanalytical and Nuclear Chemistry*,  
25 693 247(3): 563-566.

26 694 Lal, R., 2015. Restoring Soil Quality to Mitigate Soil Degradation. *Sustainability*, 7(5): 5875-5895.

27 695 Lal, R., Fifield, L., Tims, S., Wasson, R. and Howe, D., 2020. A study of soil erosion rates using <sup>239</sup>Pu,  
28 696 in the wet-dry tropics of northern Australia. *Journal of environmental radioactivity*, 211:  
29 697 106085.

30 698 Le Roux, G., Duffa, C., Vray, F. and Renaud, P., 2010. Deposition of artificial radionuclides from  
31 699 atmospheric Nuclear Weapon Tests estimated by soil inventories in French areas low-  
32 700 impacted by Chernobyl. *J Environ Radioact*, 101(3): 211-8.

33 701 Liddicoat, C., Maschmedt, D., Clifford, D., Searle, R., Herrmann, T., Macdonald, L.M. and Baldock, J.,  
34 702 2015. Predictive mapping of soil organic carbon stocks in South Australia's agricultural zone.  
35 703 *Soil Research*, 53(8): 956-973.

36 704 Lizaga, I., Quijano, L., Gaspar, L. and Navas, A., 2018. Estimating soil redistribution patterns with  
37 705 <sup>137</sup>Cs measurements in a Mediterranean mountain catchment affected by land  
38 706 abandonment. *Land Degradation & Development*, 29(1): 105-117.

39 707 Loughran, R., Pennock, D. and Walling, D., 2002. Spatial distribution of caesium-137, *Handbook for  
40 708 the assessment of soil erosion and sedimentation using environmental radionuclides*.  
41 709 Springer, pp. 97-109.

42 710 Mabit, L., Bernard, C., Lee Zhi Yi, A., Fulajtar, E., Dercon, G., Zaman, M., Toloza, A. and Heng, L., 2018.  
43 711 Promoting the use of isotopic techniques to combat soil erosion: An overview of the key role  
44 712 played by the SWMCN Subprogramme of the Joint FAO/IAEA Division over the last 20 years.  
45 713 *Land Degradation & Development*, 29(9): 3077-3091.

46 714 Mabit, L., Bernard, C., Makhlof, M. and Laverdière, M., 2008. Spatial variability of erosion and soil  
47 715 organic matter content estimated from <sup>137</sup>Cs measurements and geostatistics. *Geoderma*,  
48 716 145(3-4): 245-251.

49 717 Mabit, L., Meusburger, K., Fulajtar, E. and Alewell, C., 2013. The usefulness of <sup>137</sup>Cs as a tracer for  
50 718 soil erosion assessment: A critical reply to Parsons and Foster (2011). *Earth-Science Reviews*,  
51 719 127: 300-307.

- 720 Macêdo, Í.L., 2009. Estudo de modelos em ambiente de geoprocessamento para a previsão de  
1 721 erosão e assoreamento de reservatórios: O caso da bacia do Rio Indaiá – Uhe Três Marias,  
2 722 Mg. 340.
- 3 723 Malakhov, S.G. and Pudovkina, I.B., 1970. Strontium 90 fallout distribution at middle latitudes of the  
4 724 Northern and Southern Hemispheres and its relation to precipitation. *Journal of Geophysical*  
5 725 *Research*, 75(18): 3623-3628.
- 7 726 Malone, B., 2015. *ithir: Soil data and some useful associated functions*. R package version, 1.
- 8 727 Martin, P. and McBride, J.L., 2012. Radionuclide Behaviour and Transport in the Tropical Atmospheric  
9 728 Environment, *Radioactivity in the Environment*. Elsevier, pp. 59-91.
- 10 729 McBratney, A.B., Santos, M.M. and Minasny, B., 2003. On digital soil mapping. *Geoderma*, 117(1-2):  
11 730 3-52.
- 13 731 McCarthy, M., 1997. Nuclear bomb test fallout may cause many US cancers. *The Lancet*, 350(9075):  
14 732 415.
- 15 733 Mendez, M.J. and Buschiazzi, D.E., 2010. Wind erosion risk in agricultural soils under different tillage  
16 734 systems in the semiarid Pampas of Argentina. *Soil & Tillage Research*, 106(2): 311-316.
- 17 735 Meusburger, K., Evrard, O., Alewell, C., Borrelli, P., Cinelli, G., Ketterer, M., Mabit, L., Panagos, P., van  
18 736 Oost, K. and Ballabio, C., 2020. Plutonium aided reconstruction of caesium atmospheric  
20 737 fallout in European topsoils. *Scientific Reports*, 10(1).
- 21 738 Meusburger, K., Mabit, L., Ketterer, M., Park, J.-H., Sandor, T., Porto, P. and Alewell, C., 2016. A multi-  
22 739 radionuclide approach to evaluate the suitability of <sup>239+240</sup>Pu as soil erosion tracer. *Science*  
23 740 *of the Total Environment*, 566: 1489-1499.
- 25 741 Minasny, B. and McBratney, A.B., 2006. A conditioned Latin hypercube method for sampling in the  
26 742 presence of ancillary information. *Computers & Geosciences*, 32(9): 1378-1388.
- 27 743 Minella, J.P., Walling, D.E. and Merten, G.H., 2014. Establishing a sediment budget for a small  
28 744 agricultural catchment in southern Brazil, to support the development of effective sediment  
29 745 management strategies. *Journal of Hydrology*, 519: 2189-2201.
- 30 746 Montes, M., Silva, L., Sá, C., Runco, J., Taylor, M. and Desimoni, J., 2013. Inventories and  
32 747 concentration profiles of <sup>137</sup>Cs in undisturbed soils in the northeast of Buenos Aires  
33 748 Province, Argentina. *Journal of environmental radioactivity*, 116: 133-140.
- 34 749 Montgomery, D.R., 2007. Soil erosion and agricultural sustainability. *Proceedings of the National*  
35 750 *Academy of Sciences*, 104(33): 13268-13272.
- 36 751 Navas, A., Machín, J. and Soto, J., 2005. Assessing soil erosion in a Pyrenean mountain catchment  
38 752 using GIS and fallout <sup>137</sup>Cs. *Agriculture, Ecosystems & Environment*, 105(3): 493-506.
- 39 753 Navas, A., Serrano, E., López-Martínez, J., Gaspar, L. and Lizaga, I., 2018. Interpreting environmental  
40 754 changes from radionuclides and soil characteristics in different landform contexts of  
41 755 Elephant Island (maritime Antarctica). *Land Degradation & Development*, 29(9): 3141-3158.
- 42 756 Owens, P., Batalla, R., Collins, A., Gomez, B., Hicks, D., Horowitz, A., Kondolf, G., Marden, M., Page,  
43 757 M. and Peacock, D., 2005. Fine-grained sediment in river systems: environmental significance  
45 758 and management issues. *River research and applications*, 21(7): 693-717.
- 46 759 Owens, P.N. and Walling, D.E., 1996. Spatial variability of caesium-137 inventories at reference sites:  
47 760 an example from two contrasting sites in England and Zimbabwe. *Applied Radiation and*  
48 761 *Isotopes*, 47(7): 699-707.
- 49 762 Palsson, S.E., Howard, B.J. and Wright, S.M., 2006. Prediction of spatial variation in global fallout of  
50 763 <sup>137</sup>Cs using precipitation. *Sci Total Environ*, 367(2-3): 745-56.
- 52 764 Panagos, P., Borrelli, P., Poesen, J., Ballabio, C., Lugato, E., Meusburger, K., Montanarella, L. and  
53 765 Alewell, C., 2015. The new assessment of soil loss by water erosion in Europe. *Environmental*  
54 766 *Science & Policy*, 54: 438-447.
- 55 767 Panagos, P., Borrelli, P., Poesen, J., Meusburger, K., Ballabio, C., Lugato, E., Montanarella, L. and  
56 768 Alewell, C., 2016. Reply to the comment on “The new assessment of soil loss by water  
57 769 erosion in Europe” by Fiener & Auerswald. *Environmental Science & Policy*, 57: 143-150.
- 59 770 Parsons, A.J. and Foster, I.D.L., 2011. What can we learn about soil erosion from the use of <sup>137</sup>Cs?  
60 771 *Earth-Science Reviews*, 108(1-2): 101-113.

772 Parsons, A.J. and Foster, I.D.L., 2013. The assumptions of science. *Earth-Science Reviews*, 127: 308-  
1 773 310.

2 774 Pebesma, E.J., 2018. Simple features for R: Standardized support for spatial vector data. *R J.*, 10(1):  
3 775 439.

4 776 Pennock, D., 2000. Suitability of <sup>137</sup>Cs redistribution as an indicator of soil quality. *Acta geológica*  
5 777 *hispanica*: 213-217.

7 778 Porto, P., Walling, D.E., Callegari, G. and Capra, A., 2009. Using caesium-137 and unsupported lead-  
8 779 <sup>210</sup>Pb measurements to explore the relationship between sediment mobilisation, sediment  
9 780 delivery and sediment yield for a Calabrian catchment. *Marine and Freshwater research*,  
10 781 60(7): 680-689.

11 782 Quinton, J.N., Govers, G., Van Oost, K. and Bardgett, R.D., 2010. The impact of agricultural soil  
12 783 erosion on biogeochemical cycling. *Nature Geoscience*, 3(5): 311-314.

14 784 Racoviteanu, A., 2007. GLIMS Glacier Database, Version 1. Analysis IDs 60827-61235, Accessed  
15 785 1/17/2017.

16 786 Ritchie, J. and Ritchie, C., 2007. Bibliography of Publications of <sup>137</sup>Cesium Studies Related to Erosion  
17 787 and Sediment Deposition. Hydrology and Remote Sensing Laboratory, Beltsville, USA.

18 788 Ritchie, J.C. and McHenry, J.R., 1990. Application of Radioactive Fallout Cesium-137 for Measuring  
19 789 Soil Erosion and Sediment Accumulation Rates and Patterns: A Review. *Journal of*  
20 790 *Environment Quality*, 19(2): 215.

22 791 Rossel, R.V., Chen, C., Grundy, M., Searle, R., Clifford, D. and Campbell, P., 2015. The Australian  
23 792 three-dimensional soil grid: Australia's contribution to the GlobalSoilMap project. *Soil*  
24 793 *Research*, 53(8): 845-864.

26 794 Roudier, P., 2011. *clhs*: a R package for conditioned Latin hypercube sampling. R package version 0.5-  
27 795 1.

28 796 Schuller, P., Bunzl, K., Voigt, G., Ellies, A. and Castillo, A., 2003a. Global fallout <sup>137</sup>Cs accumulation  
29 797 and vertical migration in selected soils from South Patagonia. *Journal of Environmental*  
30 798 *Radioactivity*, 71(1): 43-60.

32 799 Schuller, P., Ellies, A., Castillo, A. and Salazar, I., 2003b. Use of <sup>137</sup>Cs to estimate tillage- and water-  
33 800 induced soil redistribution rates on agricultural land under different use and management in  
34 801 central-south Chile. *Soil & Tillage Research*, 69(1-2): 69-83.

35 802 Schuller, P., Voigt, G., Handl, J., Ellies, A. and Oliva, L., 2002. Global weapons' fallout <sup>137</sup>Cs in soils  
36 803 and transfer to vegetation in south-central Chile. *Journal of Environmental Radioactivity*,  
37 804 62(2): 181-193.

39 805 Simon, S.L., Bouville, A. and Land, C.E., 2006. Fallout from nuclear weapons tests and cancer risks:  
40 806 exposures 50 years ago still have health implications today that will continue into the future.  
41 807 *American Scientist*, 94(1): 48-57.

42 808 Steffen, W., Broadgate, W., Deutsch, L., Gaffney, O. and Ludwig, C., 2015. The trajectory of the  
43 809 Anthropocene: the great acceleration. *The Anthropocene Review*, 2(1): 81-98.

45 810 Steinhäuser, G., Brandl, A. and Johnson, T.E., 2014. Comparison of the Chernobyl and Fukushima  
46 811 nuclear accidents: a review of the environmental impacts. *Sci Total Environ*, 470-471: 800-17.

47 812 Tagami, K., Tsukada, H. and Uchida, S., 2019. Quantifying spatial distribution of <sup>137</sup>Cs in reference  
48 813 site soil in Asia. *CATENA*, 180: 341-345.

49 814 Tamura, T., 1961. Cesium sorption reactions as indicator of clay mineral structures. *Clays and Clay*  
50 815 *Minerals*, 10(1): 389-398.

52 816 Tamura, T. and Jacobs, D., 1960. Structural implications in cesium sorption. *Health physics*, 2(4): 391-  
53 817 398.

54 818 Tassano, M., Montañez, A., Nuñez, L., Trasante, T., González, J., Irigoyen, J., Cabral, P. and Cabrera,  
55 819 M., 2020. Spatial cross-correlation between physicochemical and microbiological variables at  
56 820 superficial soil with different levels of degradation. *CATENA*: 105000.

58 821 Team R Core, 2013. *R: A language and environment for statistical computing*. Vienna, Austria.

59 822 Tenenhaus, M., 1998. *La régression PLS: théorie et pratique*. Editions technip.

823 Turney, C.S.M., Palmer, J., Maslin, M.A., Hogg, A., Fogwill, C.J., Southon, J., Fenwick, P., Helle, G.,  
1 824 Wilmshurst, J.M., McGlone, M., Bronk Ramsey, C., Thomas, Z., Lipson, M., Beaven, B., Jones,  
2 825 R.T., Andrews, O. and Hua, Q., 2018. Global Peak in Atmospheric Radiocarbon Provides a  
3 826 Potential Definition for the Onset of the Anthropocene Epoch in 1965. *Scientific Reports*,  
4 827 8(1): 3293.

5 828 UNSCEAR, 1962. Report of the United Nations Scientific Committee on the effects of atomic  
6 829 radiation. Annex F : Environmental contamination, New York.

7 830 UNSCEAR, 2000. Effects of Ionizing Radiation. United Nations, New York: 453-487.

8 831 UNSCEAR, 2008. Sources and effects of ionizing radiation: United Nations Scientific Committee on the  
9 832 Effects of Atomic Radiation: UNSCEAR 2008 report to the General Assembly, with scientific  
10 833 annexes. United Nations, New York.

11 834 Vanwalleghem, T., Gómez, J.A., Infante Amate, J., González de Molina, M., Vanderlinden, K., Guzmán,  
12 835 G., Laguna, A. and Giráldez, J.V., 2017. Impact of historical land use and soil management  
13 836 change on soil erosion and agricultural sustainability during the Anthropocene.  
14 837 *Anthropocene*, 17: 13-29.

15 838 Volchok, H., 1965. Distribution of strontium-90 in surface air during 1963. *Nature*, 206(4988): 1031-  
16 839 1033.

17 840 Volchok, H., 1966. The global strontium 90 budget. *Journal of Geophysical Research*, 71(6): 1515-  
18 841 1518.

19 842 Wadoux, A.M.-C., Brus, D.J. and Heuvelink, G.B., 2019. Sampling design optimization for soil mapping  
20 843 with random forest. *Geoderma*, 355: 113913.

21 844 Walling, D. and He, Q., 2000. The global distribution of bomb-derived <sup>137</sup>Cs reference inventories.  
22 845 Final report on IAEA technical contract, 10361: 1-11.

23 846 Walling, D., Zhang, Y. and He, Q., 2011. Models for deriving estimates of erosion and deposition rates  
24 847 from fallout radionuclide (caesium-137, excess lead-210, and beryllium-7) measurements  
25 848 and the development of user friendly software for model implementation. Impact of soil  
26 849 conservation measures on erosion control and soil quality. IAEA-TECDOC-1665: 11-33.

27 850 Walling, D.E. and Quine, T., 1990. Calibration of caesium-137 measurements to provide quantitative  
28 851 erosion rate data. *Land Degradation & Development*, 2(3): 161-175.

29 852 Wei, T., Simko, V., Levy, M., Xie, Y., Jin, Y. and Zemla, J., 2017. Package 'corrplot'. *Statistician*,  
30 853 56(316): e24.

31 854 Wickham, H., 2016. *ggplot2: elegant graphics for data analysis*. springer.

32 855 Wingeyer, A.B., Amado, T.J.C., Perez-Bidegain, M., Studdert, G.A., Varela, C.H.P., Garcia, F.O. and  
33 856 Karlen, D.L., 2015. Soil Quality Impacts of Current South American Agricultural Practices.  
34 857 *Sustainability*, 7(2): 2213-2242.

35 858 Wright, S.M., Howard, B.J., Strand, P., Nylén, T. and Sickel, M.A.K., 1999. Prediction of <sup>137</sup>Cs  
36 859 deposition from atmospheric nuclear weapons tests within the Arctic. *Environmental  
37 860 Pollution*, 104(1): 131-143.

38 861 Zapata, F., 2002. Handbook for the assessment of soil erosion and sedimentation using  
39 862 environmental radionuclides, 219. Springer.

40 863 Zapata, F., 2003. The use of environmental radionuclides as tracers in soil erosion and sedimentation  
41 864 investigations: recent advances and future developments. *Soil and Tillage Research*, 69(1-2):  
42 865 3-13.

51 866  
52  
53  
54  
55  
56  
57  
58  
59  
60  
61  
62  
63  
64  
65

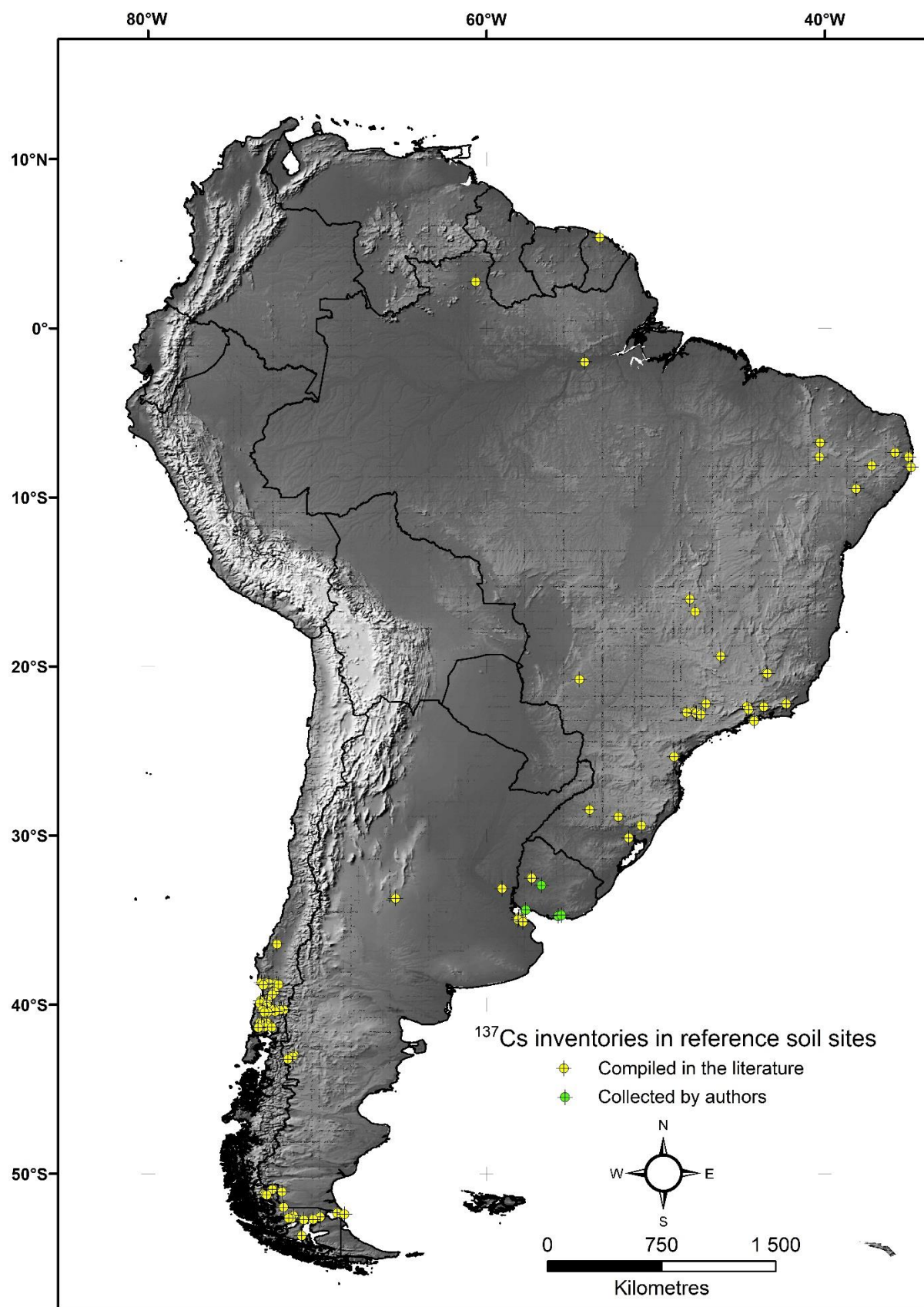


**Figure 1:** Spatial distribution of  $^{137}\text{Cs}$  reference soil sites in undisturbed soil profiles of South America as documented in the literature and collected by the authors.

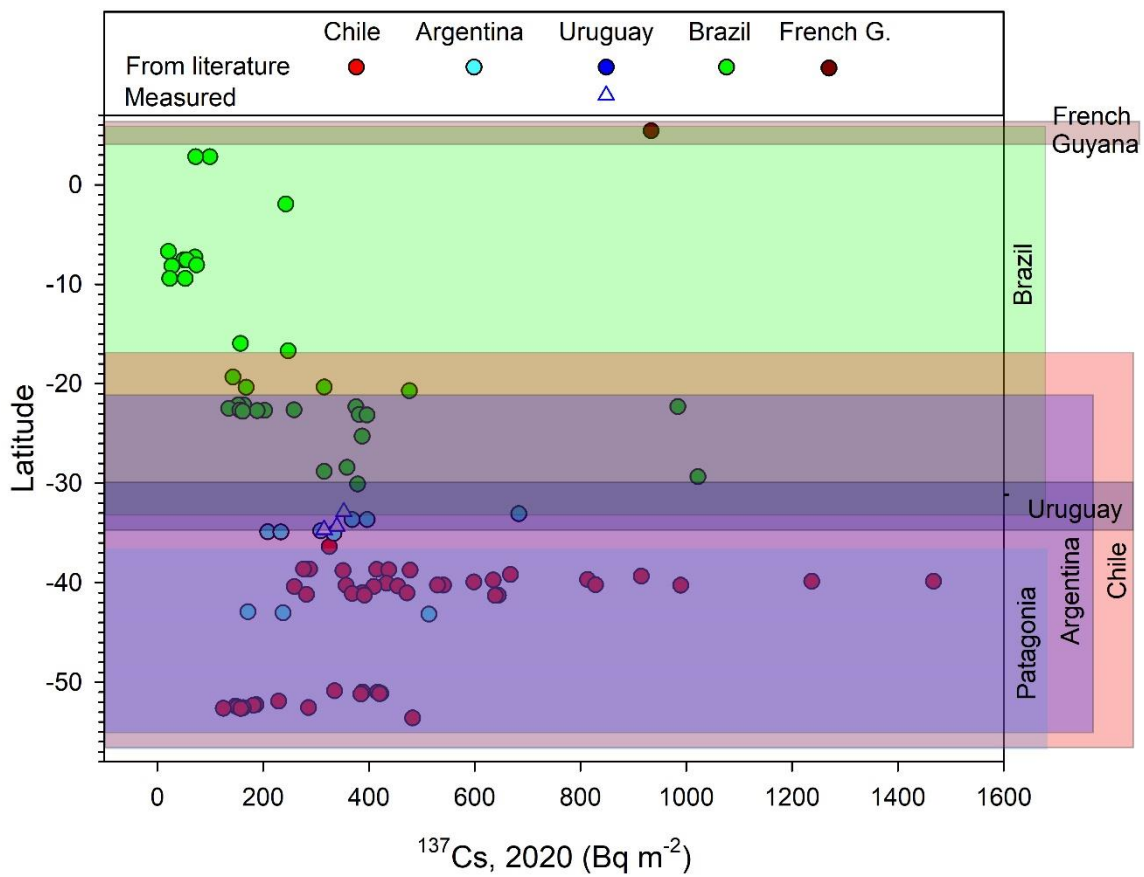


**Figure 2:** Variation of  $^{137}\text{Cs}$  inventories in reference soil sites ( $\text{Bq m}^{-2}$ ), decay-corrected to 2020 and plotted against south latitude.

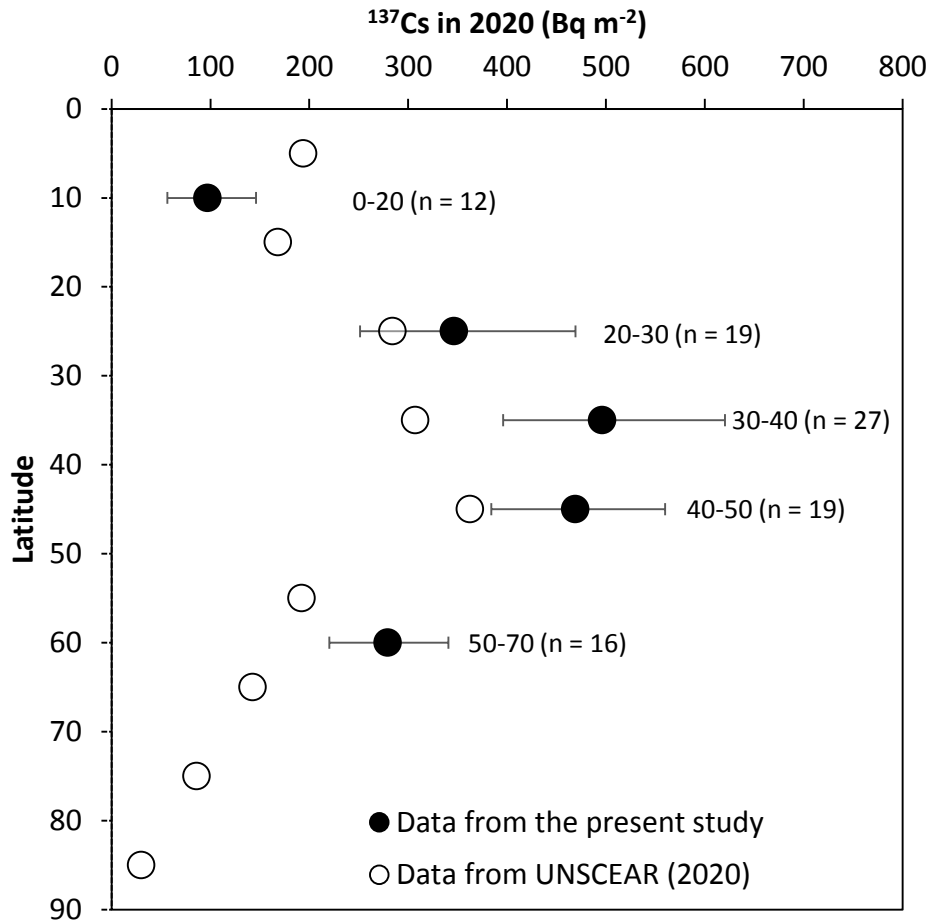


**Figure 3:** Distribution of mean  $^{137}\text{Cs}$  in reference soil sites documented in our review for each  $10^\circ$  latitude bands compared with the distribution of radionuclide fallout from thermonuclear bomb testing with latitude, after UNSCEAR (2000). This distribution was calculated with 5000 samples generated using bootstrap iterations; the circle is the calculated mean while the whiskers represent the 95% confident interval.

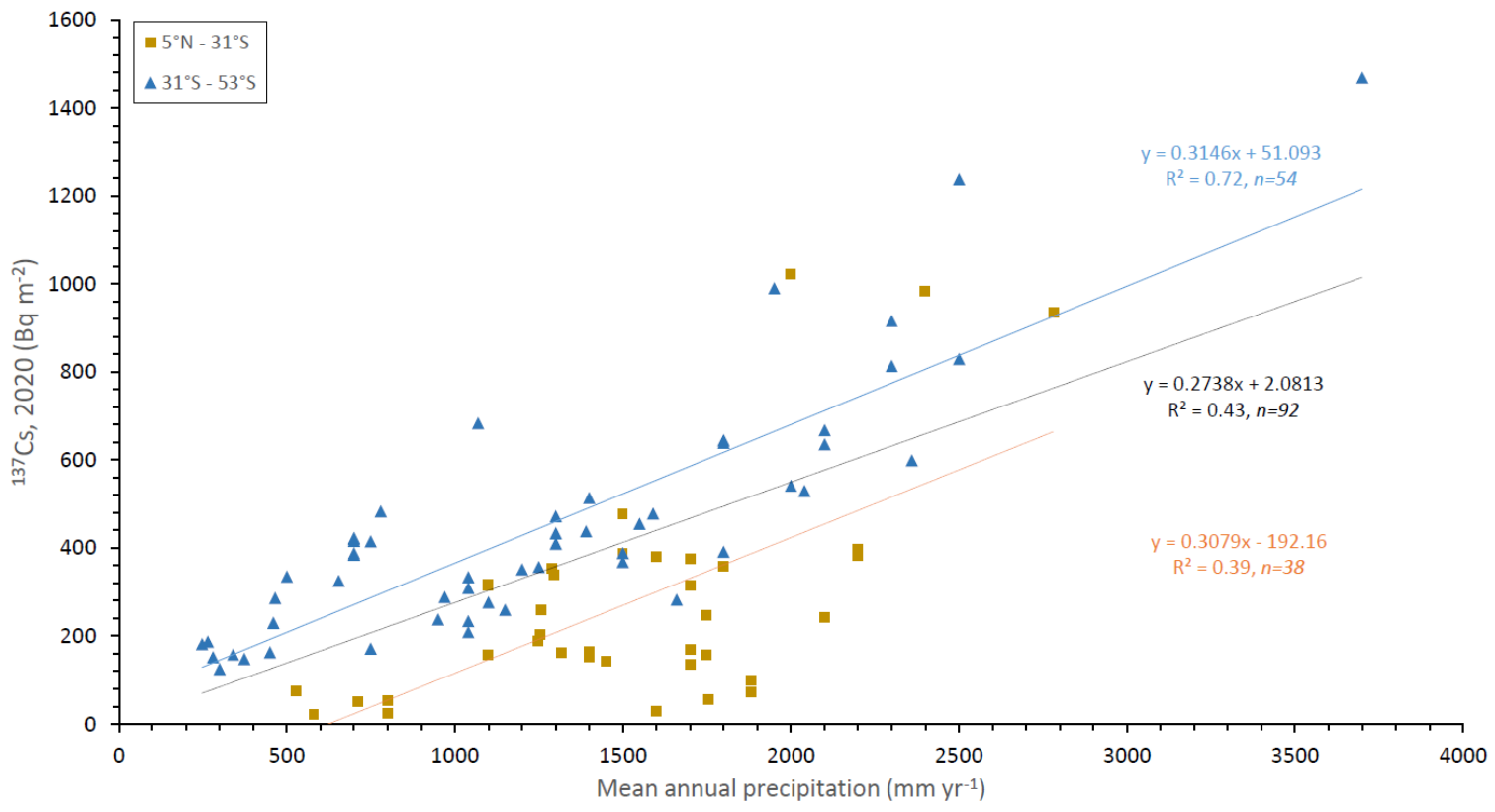


**Figure 4:** Relationships between mean annual precipitation and  $^{137}\text{Cs}$  inventories in reference soil sites for different latitude ranges.

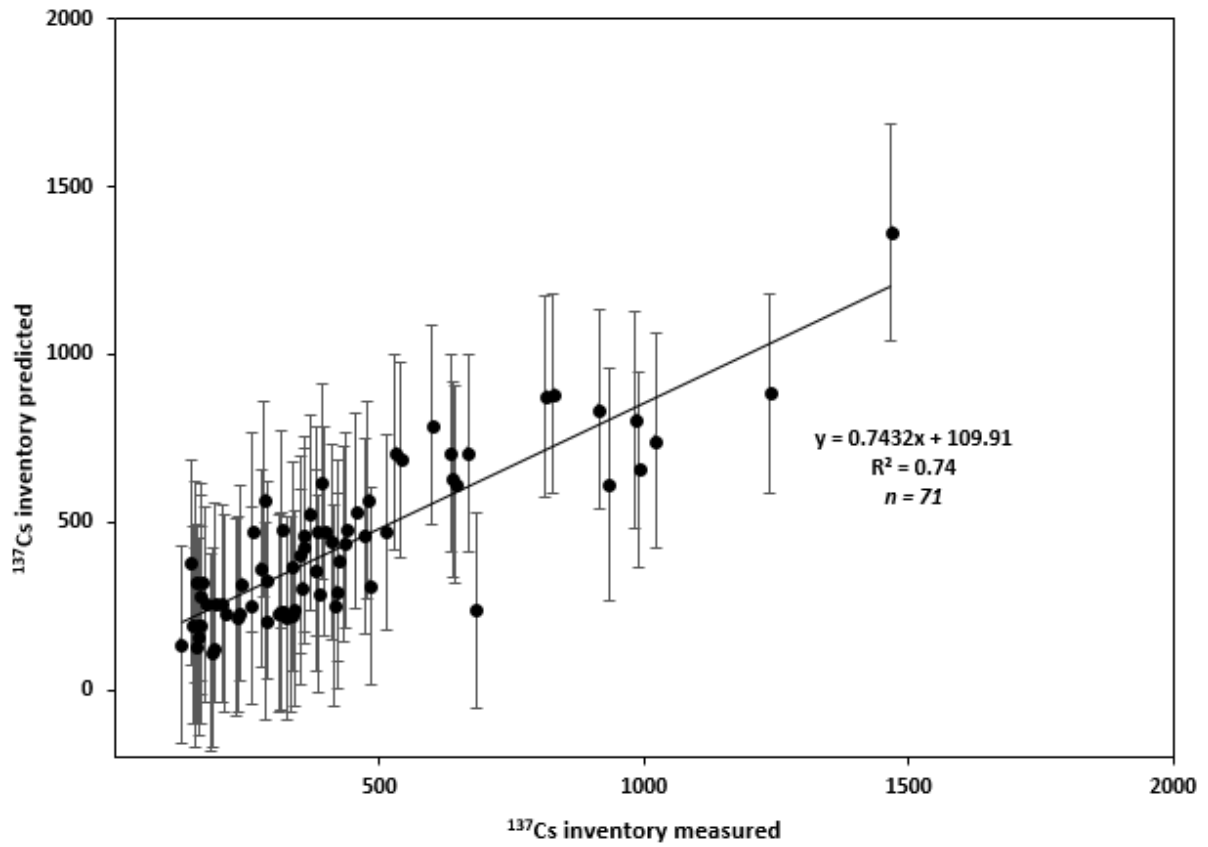


**Figure 5:** Results of the multiple regressions using latitude, longitude, elevation and rainfall plotted with the 95% confidence intervals.

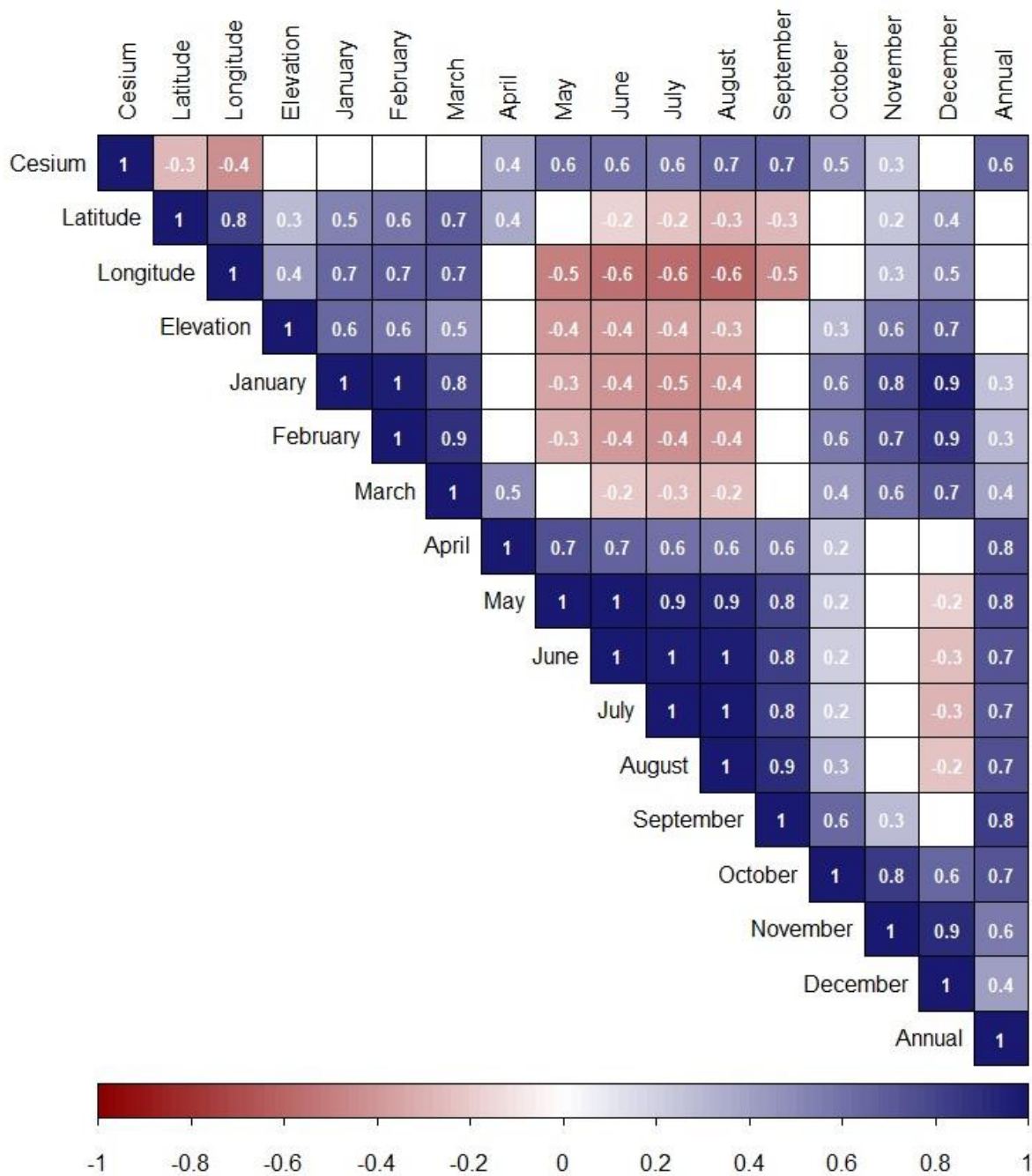


**Figure 6:** Correlogram plot for  $^{137}\text{Cs}$  inventories in reference soil sites, mean monthly/annual precipitation rates (1950-2000) and geographical information. Significant levels  $> 0.1$  are represented as white squares.

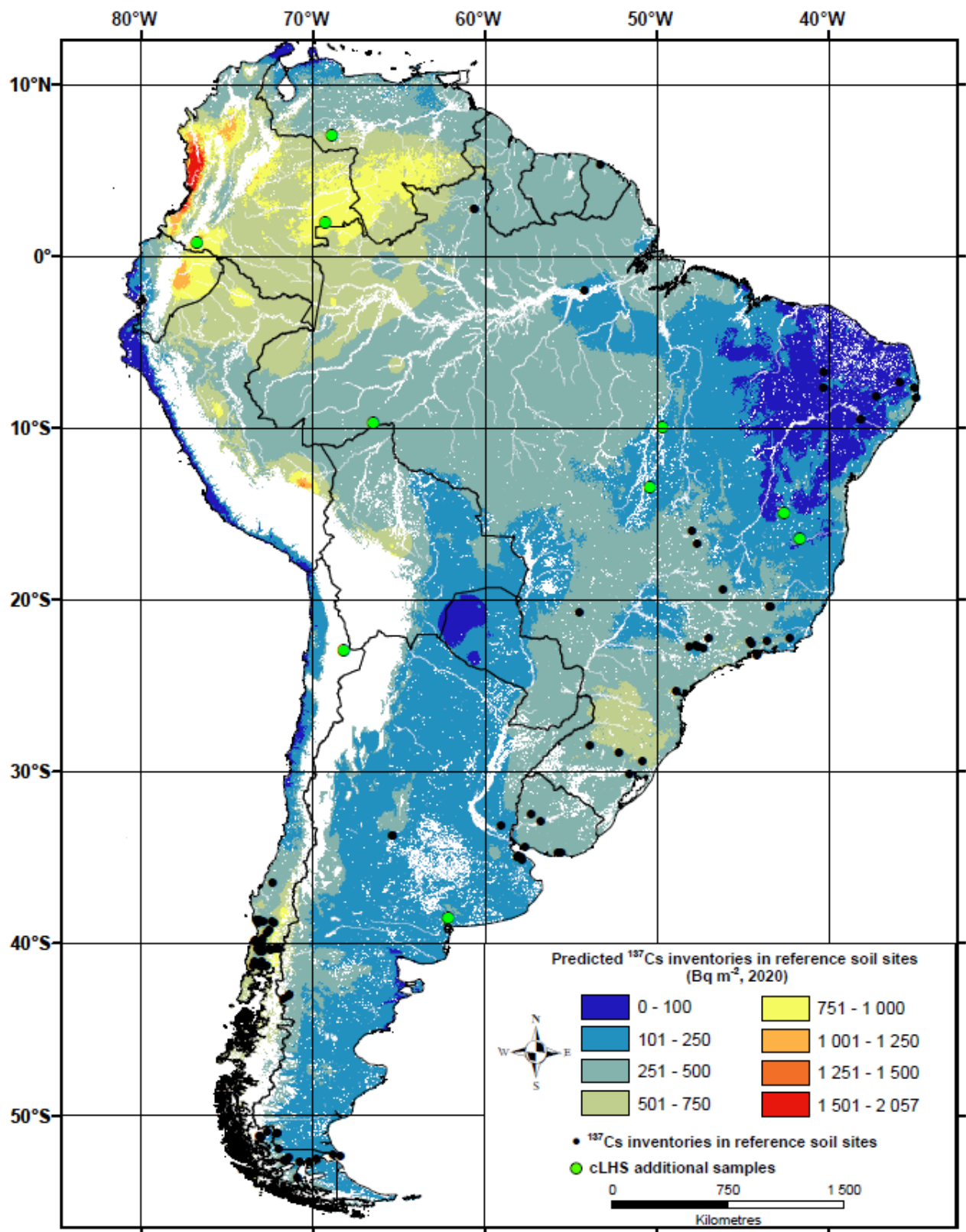


**Figure 7:** Baseline  $^{137}\text{Cs}$  inventories in reference soil sites ( $\text{Bq m}^{-2}$ , 2020) estimated by Partial Least Square Regression (PLSR) with a spatial resolution of 2 km. Black dots represent those  $^{137}\text{Cs}$  inventories compiled in the literature and measured by the authors, while green dots represent the additional samples that should be analysed in the future as determined by conditioned Latin Hypercube Sampling (cLHS) to improve model quality. Areas above 1,800 m a.s.l., glaciers and large water bodies have been masked in white using the GMTED2010 30-arc-second elevation database (Danielson and Gesch, 2011) and the GLIMS glacier database (Racoviteanu, 2007).

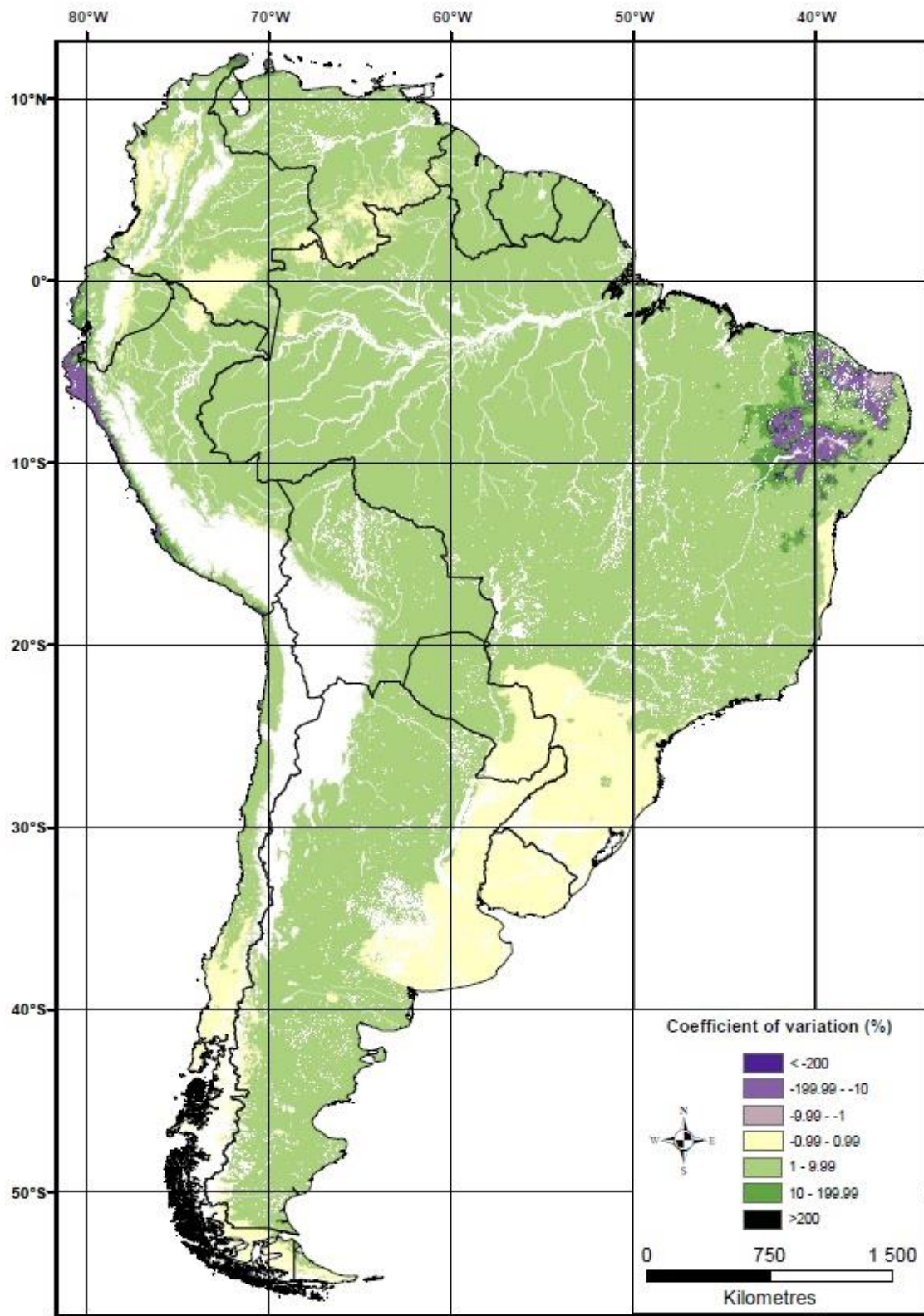


**Figure 8:** Prediction uncertainties of the baseline map of  $^{137}\text{Cs}$  inventories in reference soil sites assessed through a non-parametric bootstrap approach ( $n=100$  contributing predictions). Areas above 1,800 m a.s.l., glaciers and large water bodies have been masked in white using the GMTED2010 30-arc-second elevation database (Danielson and Gesch, 2011) and the GLIMS glacier database (Racoviteanu, 2007).

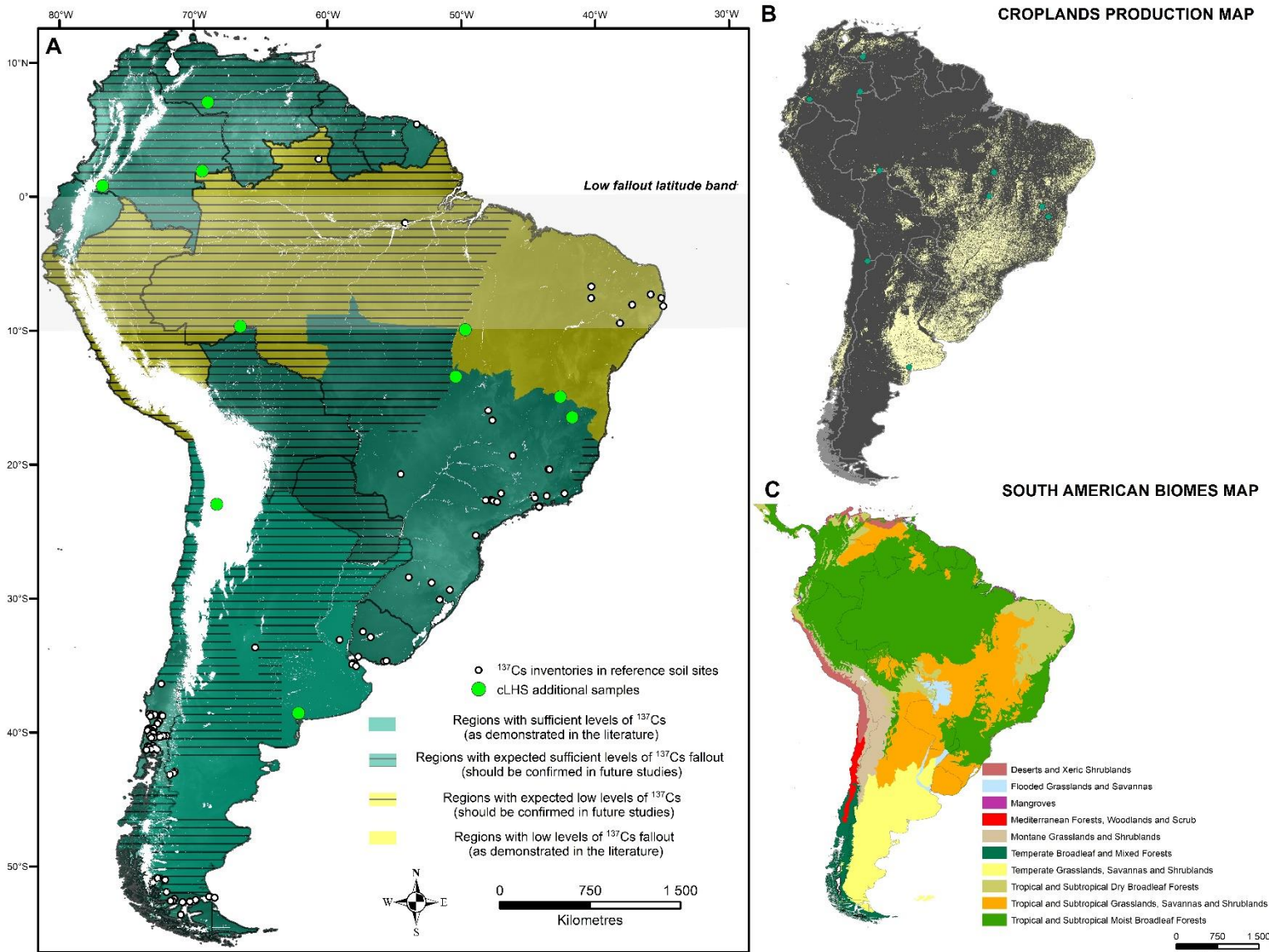


**Figure 9:** (A) Potential use of  $^{137}\text{Cs}$  fallout inventories for Earth Science applications in South America. Areas above 1,800 m a.s.l., glaciers and large water bodies have been masked in white using the GMTED2010 30-arc-second elevation database (Danielson and Gesch, 2011) and the GLIMS glacier database (Racoviteanu, 2007). (B) cropland distribution across South America in a nominal 30-meter resolution (GFSAD30 Project), and (C) terrestrial biomes of South America (Dinerstein et al., 2017)